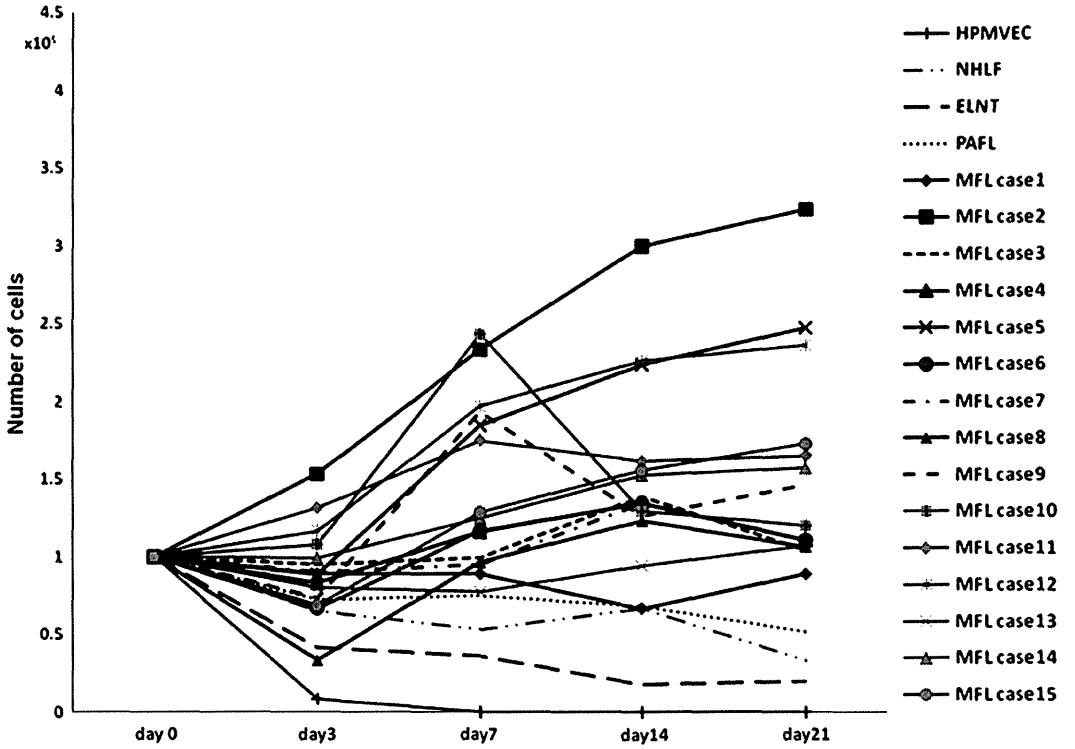

Fig. 5. Serum starvation. Comparison of the growth of HPMVEC, NHLF, PAFL and MFL in the absence of serum. Cells at passage 4 were seeded at 1×10^5 in the 25 cm^2 flasks at day 0 and were incubated with serum-free medium for the incubation period. At each indicated day, a flask was trypsinized and the cells counted. The average values of 3 experiments are shown. *Definition of abbreviations:* HPMVEC = Human pulmonary microvascular endothelial cells; NHLF = Normal Human Lung Fibroblast; ELNT = endothelial-like cells from the neighbor tissue; MFL = myofibroblast-like cells; PAFL = pulmonary arterial fibroblast-like cells.

Ministry of Health, Labor and Welfare, Japan and a Grant-in-Aid for Scientific Research (Category C 22590851) from the Japanese Ministry of Education and Science.

The authors of this manuscript have certified that they comply with the principles of ethical publishing in the International Journal of Cardiology [42].

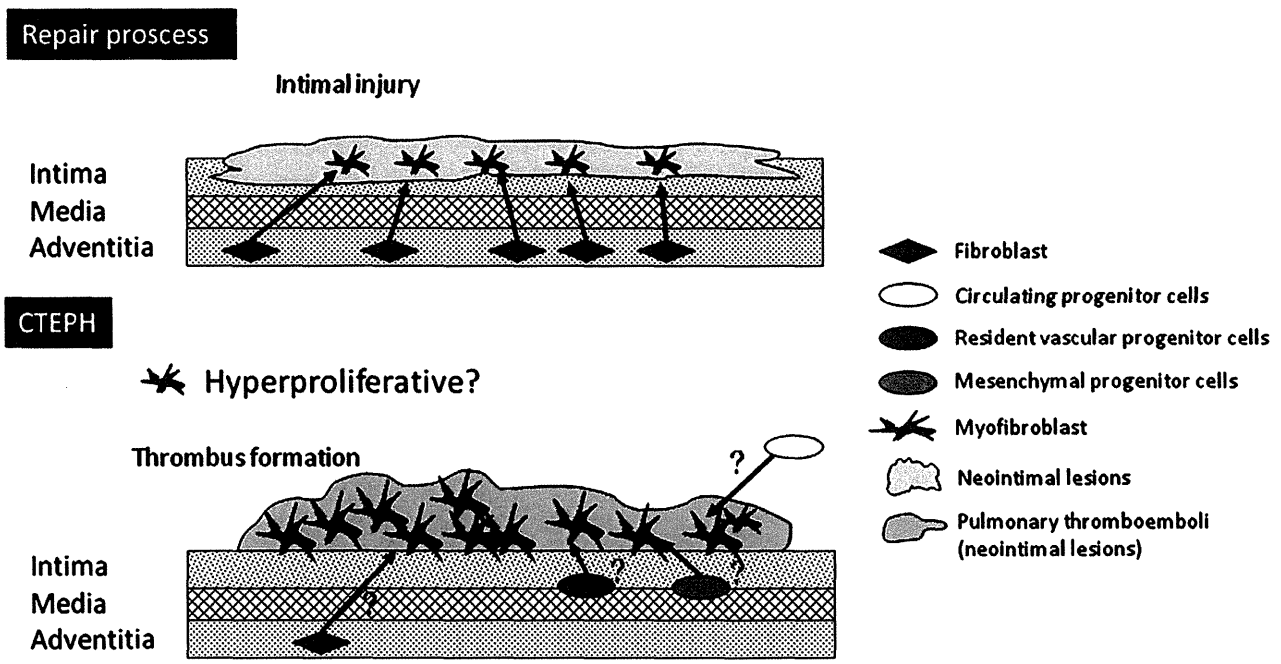

Fig. 6. A hypothetical mechanism of Thromboemboli (neointimal lesions) in CTEPH. In normal repair process, after intimal injury fibroblasts migrate to intima and transdifferentiate into contractile and secretory myofibroblasts. After formation of neointima, they apotose and disappear. In CTEPH, after thrombus formation, probably fibroblasts, circulating progenitor cells and/or resident vascular progenitor cells and/or mesenchymal progenitor cells may transdifferentiate or dysregulated differentiate into myofibroblasts and their hyperproliferative state may result in fibrinolysis-resident neointima.

References

[1] Fedullo PF, Kerr KM, Auger WR, Jamieson SW, Kapelanski DP. Chronic thromboembolic pulmonary hypertension. Semin Respir Crit Care Med 2000;21:563–74.
[2] Moser KM, Daily PO, Peterson K, et al. Thromboendarterectomy for chronic, major vessel thromboembolic pulmonary hypertension: immediate and long-term results in 42 patients. Ann Intern Med 1987;107:560–5.
[3] Egermayer P, Peacock AJ. Is pulmonary embolism a common cause of chronic pulmonary hypertension? Limitations of the embolic hypothesis. Eur Respir J 2000;15:440–8.
[4] Hoeper MM, Mayer E, Simonneau G, Rubin L. Chronic thromboembolic pulmonary hypertension. Circulation 2006;113:2011–20.
[5] Dartevelle P, Fadel E, Mussot S, et al. Chronic thromboembolic pulmonary hypertension. Eur Respir J 2004;23:637–48.
[6] Galiè N, Kim NHS. Pulmonary microvascular disease in chronic thromboembolic pulmonary hypertension. Proc Am Thorac Soc 2006;3:571–6.
[7] Fedullo PF, Rubin LJ, Kerr KM, Auger WR, Channick RN. The natural history of acute and chronic thromboembolic disease: the search for the missing link. Eur Respir J 2000;15:435–7.
[8] Mayer E. Surgical and post-operative treatment of chronic thromboembolic pulmonary hypertension. Eur Respir Rev 2010;19:64–7.
[9] Freed DH, Thomson BM, Berman M, et al. Survival after pulmonary thromboendarterectomy: effect of residual pulmonary hypertension. J Thorac Cardiovasc Surg 2011;141:383–7.
[10] Wolf M, Boyer-Neumann C, Parent F, et al. Thrombotic risk factors in pulmonary hypertension. Eur Respir J 2000;15:395–9.
[11] Morris TA, Marsh JJ, Chiles PG, Auger WR, Fedullo PF, Woods Jr VL. Fibrin derived from patients with chronic thromboembolic pulmonary hypertension is resistant to lysis. Am J Respir Crit Care Med 2006;173:1270–5.
[12] Suntharalingam J, Goldsmith K, van Marion V, et al. Fibrinogen Aalpha Thr312Ala polymorphism is associated with chronic thromboembolic pulmonary hypertension. Eur Respir J 2008;31:736–41.
[13] Morris TA, Marsh JJ, Chiles PG, et al. High prevalence of dysfibrinogenemia among patients with chronic thromboembolic pulmonary hypertension. Blood 2009;114: 1929–36.
[14] Matsuda M, Sugo T. Structure and function of human fibrinogen inferred from dysfibrinogens. Int J Hematol 2002;76:352–60.
[15] Yi ES, Kim H, Ahn H, et al. Distribution of obstructive intimal lesions and their cellular phenotypes in chronic pulmonary hypertension. A morphometric and immunohistochemical study. Am J Respir Crit Care Med 2000;162:1577–86.
[16] Blauwet LA, Edwards WD, Tazelaar HD, McGregor CG. Surgical pathology of pulmonary thromboendarterectomy: a study of 54 cases from 1990 to 2001. Hum Pathol 2003;34:1290–8.
[17] Hinz B, Phan SH, Thannickal VJ, Galli A, Bochaton-Piallat ML, Gabbiani G. The myofibroblast: one function, multiple origins. Am J Pathol 2007;170:1807–16.
[18] De Wever O, Mareel M. Role of tissue stroma in cancer cell invasion. J Pathol 2003;200:429–47.
[19] Sakao S, Taraseviciene-Stewart L, Cool CD, et al. VEGF-R blockade causes endothelial cell apoptosis, expansion of surviving CD34+ precursor cells and transdifferentiation to smooth muscle-like and neuronal-like cells. FASEB J 2007;21:3640–52.
[20] Sakao S, Taraseviciene-Stewart L, Lee JD, Wood K, Cool CD, Voelkel NF. Initial apoptosis is followed by increased proliferation of apoptosis-resistant endothelial cells. FASEB J 2005;19:1178–80.
[21] Sakao S, Hashimoto T, Shino Y, et al. Expression of the potential novel gene E6DG1 downregulated by the E6 protein of human papillomavirus type 16 is correlated with anchorage-independent growth. Int J Oncol 2002;21:273–9.
[22] Bonderman D, Wilkens H, Wakounig S, et al. Risk factors for chronic thromboembolic pulmonary hypertension. Eur Respir J 2009;33:325–31.
[23] Freedman VH, Shin S. Cellular tumorigenicity in nude mice: correlation with cell growth in semisolid medium. Cell 1974;3:355–9.
[24] Wang W, Goswami S, Sahai E, Wyckoff JB, Segall JE, Condeelis JS. Tumor cells caught in the act of invading: their strategy for enhanced cell motility. Trends Cell Biol 2005;15:138–45.
[25] Hanahan D, Weinberg R. The hallmarks of cancer. Cell 2000;100:57–70.
[26] Tomasek JJ, Gabbiani G, Hinz B, Chaponnier C, Brown RA. Myofibroblasts and mechano-regulation of connective tissue remodeling. Nat Rev Mol Cell Biol 2002;3:349–63.
[27] Carlson MA, Longaker MT, Thompson JS. Wound splinting regulates granulation tissue survival. J Surg Res 2003;110:304–9.
[28] Thannickal VJ, Toews GB, White ES, Lynch III JP, Martinez FJ. Mechanisms of pulmonary fibrosis. Annu Rev Med 2004;55:395–417.
[29] Desmoulière A, Darby IA, Gabbiani G. Normal and pathologic soft tissue remodeling: role of the myofibroblast, with special emphasis on liver and kidney fibrosis. Lab Investig 2003;83:1689–707.
[30] Zalewski A, Shi Y, Johnson AG. Diverse origin of intimal cells: smooth muscle cells, myofibroblasts, fibroblasts, and beyond? Circ Res 2002;91:652–5.
[31] Hao H, Gabbiani G, Camenzind E, Bacchetta M, Virmani R, Bochaton-Piallat ML. Phenotypic modulation of intima and media smooth muscle cells in fatal cases of coronary artery lesion. Arterioscler Thromb Vasc Biol 2006;26:326–32.
[32] Yao Weijuan, Firth Amy L, Sacks Richard S, et al. Identification of putative endothelial progenitor cells ($CD34^+CD133^+Flk\text{-}1^+$) in endarterectomized tissue of patients with chronic thromboembolic pulmonary hypertension. Am J Physiol Lung Cell Mol Physiol 2009;296:L870–8.
[33] Firth Amy L, Yao Weijuan, Ogawa Aiko, Madani Michael M, Lin Grace Y, Yuan Jason X-J. Multipotent mesenchymal progenitor cells are present in endaretectomized tissues from patients with chronic thromboembolic pulmonary hypertension. Am J Physiol Cell Physiol 2010;298:C1217–25.
[34] Pengo V, Lensing AW, Prins MH, et al. Thromboembolic Pulmonary Hypertension Study Group. Incidence of chronic thromboembolic pulmonary hypertension after pulmonary embolism. N Engl J Med 2004;350:2257–64.
[35] Lang I. Advances in understanding the pathogenesis of chronic thromboembolic pulmonary hypertension. Br J Haematol 2010;149:478–83.
[36] Ogawa Aiko, Firth Amy L, Yao Weijuan, et al. Inhibition of mTOR attenuates store-operated Ca2 entry in cells from endarterectomized tissues of patients with chronic thromboembolic pulmonary hypertension. Am J Physiol Lung Cell Mol Physiol 2009;297:666–76.
[37] Das M, Burns N, Wilson SJ, Zawada WM, Stenmark KR. Hypoxia exposure induces the emergence of fibroblasts lacking replication repressor signals of PKCzeta in the pulmonary artery adventitia. Cardiovasc Res 2008;78:440–8.
[38] Rai PR, Cool CD, King JA, et al. The cancer paradigm of severe angioproliferative pulmonary hypertension. Am J Respir Crit Care Med 2008;178:558–64.
[39] Sakao S, Tatsumi K. Vascular remodeling in pulmonary arterial hypertension: multiple cancer-like pathways and possible treatment modalities. Int J Cardiol 2011;147:4–12.
[40] Falati S, Liu Q, Gross P, et al. Accumulation of tissue factor into developing thrombi in vivo is dependent upon microparticle P-selectin glycoprotein ligand 1 and platelet P-selectin. J Exp Med 2003;197:1585–98.
[41] Morel O, Toti F, Hugel B, et al. Procoagulant microparticles: disrupting the vascular homeostasis equation? Arterioscler Thromb Vasc Biol 2006;26:2594–604.
[42] Shewan LG, Coats AJ. Ethics in the authorship and publishing of scientific articles. Int J Cardiol 2010;144:1–2.

Interaction and cross-resistance of cisplatin and pemetrexed in malignant pleural mesothelioma cell lines

MIYAKO KITAZONO-SAITOH[1], YUICHI TAKIGUCHI[2], SATORU KITAZONO[1], HIRONORI ASHINUMA[1], ATSUSHI KITAMURA[1], YUJI TADA[1], KATSUSHI KUROSU[1], EMIKO SAKAIDA[2], IKUO SEKINE[2], NOBUHIRO TANABE[1], MASATOSHI TAGAWA[3] and KOICHIRO TATSUMI[1]

Departments of [1]Respirology and [2]Medical Oncology, Graduate School of Medicine, Chiba University; [3]Division of Pathology and Cell Therapy, Chiba Cancer Center, Chiba, Japan

Received January 30, 2012; Accepted April 13, 2012

DOI: 10.3892/or.2012.1799

Abstract. Although cisplatin and pemetrexed are key drugs in the treatment of malignant pleural mesothelioma, their drug-drug interactions, cross-resistance and resistance mechanisms in malignant pleural mesothelioma are not well understood. In the present study, the interaction of these 2 agents was determined by clonogenic assays followed by isobologram analysis of 4 human malignant pleural mesothelioma cell lines. The cell lines were exposed to the agents using a stepwise dose-escalation method to establish drug-resistant sublines. Thymidylate synthase mRNA expression was evaluated in the drug-resistant sublines. As a consequence, cisplatin and pemetrexed had synergistic effects in 3 cell lines and an additive effect in the fourth cell line. The former 3 cell lines showed similar pemetrexed sensitivity in the parental cells and their cisplatin-resistant sublines, whereas the fourth cell line exhibited cross-resistance. In contrast, cisplatin had diverse effects on pemetrexed-resistant sublines. High thymidylate synthase expression did not correlate with natural pemetrexed resistance. Elevated thymidylate synthase expression correlated with acquired pemetrexed resistance in 2 sublines. In conclusion, cisplatin and pemetrexed showed synergistic activity and no cross-resistance in 3 of the 4 malignant pleural mesothelioma cell lines, suggesting the clinical relevance of their combination in chemotherapy. Thymidylate synthase expression did not necessarily correlate with pemetrexed resistance. The information together with the experimental model presented here would be useful for further investigating therapeutic targets of malignant mesothelioma.

Correspondence to: Dr Yuichi Takiguchi, Department of Medical Oncology, Graduate School of Medicine, Chiba University, 1-8-1, Inohana, Chuo-ku, Chiba 260-8670, Japan
E-mail: takiguchi@faculty.chiba-u.jp

Key words: mesothelioma, cisplatin, pemetrexed, cross-resistance, synergism

Introduction

Malignant pleural mesothelioma (MPM), often linked to asbestos exposure, is one of the most lethal cancers with a rapidly increasing incidence. For example, the latest available data indicate that the incidence of MPM in Australia is 40 cases per million and is predicted to increase over the next 10-15 years. In Japan, 103,000 MPM-related mortalities are predicted to occur in the next 40 years, with the estimated peak in 2025 (1). The number of MPM-related deaths in the UK is expected to double from 1,500 to 3,000/year in the 20-year period from 2000 to 2020 (2). Although the latency from asbestos exposure is ~20-30 years (3), MPM shows rapid progression, especially in the later stages. It also has a poor prognosis, with a median overall survival period of 9-17 months, regardless of stage (4). A recent randomized study demonstrated a survival benefit of a cisplatin-pemetrexed chemotherapy regimen over cisplatin chemotherapy (5). Thus, the current key drugs for the disease are cisplatin and pemetrexed. Similar to most other solid cancers, MPM may recur due to acquired resistance to chemotherapeutic agents. The development of resistance to chemotherapeutic agents is a major impediment to the success of chemotherapy. In particular, since only a few active agents are available for MPM, resistance to these agents implies complete failure of chemotherapy.

Cisplatin binds to DNA and induces DNA cross-linking, which leads to DNA double- and single-strand breaks and causes cell death (6). Pemetrexed inhibits DNA and RNA synthesis by impairing the activity of at least 3 enzymes, thymidylate synthase (TS), glycinamide ribonucleotide formyltransferase (GARFT) and dihydrofolate reductase (DHFR), in the folate metabolic pathway, a critical pathway for purine and pyrimidine synthesis (7). The clinical effectiveness of 5-fluorouracil, another TS inhibitory agent, reportedly correlates with low TS activity in colorectal (8-11), gastric (12) and non-small cell carcinomas (13). Clinical observations in breast cancer (14) and MPM (15) suggest that pemetrexed may show similar phenomenon to 5-fluorouracil. In another study, forced high or low TS expression was linked to decreased or increased sensitivity to pemetrexed *in vitro*, respectively (16,17). However, the precise

interaction of pemetrexed and cisplatin in MPM remains unclear; there is no information on whether the interaction is supra-, sub- or just additive, although limited information regarding the drug-drug interactions of the 2 agents on gastric cancer (18), lung adenocarcinoma, and colorectal, breast, and ovarian cancer cell lines (19) is available. There is, however, no information on cross-resistance between the 2 agents or the precise mechanism of acquired resistance.

Therefore, elucidating the interactions and cross-resistance between cisplatin and pemetrexed, as well as the mechanism of acquired resistance, in human MPM would be crucial in improving the therapeutic strategies against the disease. In this study, the interaction of these 2 agents in 4 human MPM cell lines was assessed *in vitro* by performing clonogenic assays followed by isobologram analysis. To assess acquired resistance, we established cisplatin- and pemetrexed-resistant sublines of these human MPM cell lines by stepwise dose-escalation of the agents. These resistant sublines were used in clonogenic assays to assess cross-resistance between the agents. In addition, expression of TS, GARFT and DHFR in these sublines and their parental cell lines were evaluated to decipher the mechanism of natural and acquired resistance.

Materials and methods

Cells and cell culture. The human mesothelioma cell lines NCI-H2452 (H2452), NCI-H28 (H28), NCI-H226 (H226) and MSTO-211H (211H) were obtained from American Type Culture Collection (Rockville, MD, USA). The histological type of H2452, H28 and H226 cells was epithelial, and that of 211H was bi-phasic. A preliminary polymerase chain reaction-single strand conformation polymorphism analysis, including exons 5, 6, 7, 8 and 9 of *TP53* of the cell lines, showed that all of them had wild-type *TP53* (data not shown). These cells were cultured as a monolayer in a humidified atmosphere with 5% CO_2 at 37°C in RPMI-1640 medium (Life Technologies, Grand Island, NY, USA), supplemented with 100 U/ml of penicillin, 100 mg/ml of streptomycin and 10% heat-inactivated fetal bovine serum.

Drugs. Cisplatin solution, at a concentration of 0.5 mg/ml (pH 2.5-5.5), was purchased from Nihon Kayaku Co. (Tokyo, Japan), and pemetrexed powder was purchased from Eli Lilly Japan K.K. (Kobe, Japan). The reagents were stored protected from light at room temperature until use. Pemetrexed was dissolved in saline at a concentration of 25 mg/ml (pH 6.6-7.8) and was used within 24 h after preparation.

Clonogenic assay. For clonogenic assays, subconfluent cultured cells were trypsinized to obtain cell suspensions, and a varied number of cells, such that the resulting colony number per plate would be ~20-50, were immediately replated onto 6-cm culture dishes, in triplicate, and cultured for 24 h in the complete medium. The agents, at various concentrations, were added to the culture medium for 24 h and were then replaced with new agent-free complete medium twice, followed by further incubation for 10-14 days. The obtained colonies were counted under a dissecting microscope after 1% crystal violet staining. Survival curves were drawn on the basis of the obtained data.

Isobologram analysis. Cell-survival curves with cisplatin, pemetrexed and their admixtures were analyzed by obtaining isobolograms according to the method described by Steel and Peckham (20). Briefly, mode I and II curves were drawn by calculating the additive response for the 2 agents using their individual survival curves. The mode I and II curves were assumed to represent complete independence of the agents, and exact complementation of the effect of one by the other, respectively. Isobologram analyses were carried out for 2 end-points, representing survival fractions of 0.05 and 0.02. First, cell killing by cisplatin was read off the cisplatin-alone survival curve. Then, the pemetrexed concentration required to kill the remaining cells to reach the end-point was read off the pemetrexed-alone survival curve. This was done by starting either at 100% survival (mode I) or at the survival already reached after cisplatin pretreatment (mode II), to form the isobologram envelope. Then, the actual data from the combination of the 2 agents were plotted on the isobologram envelope. Data points in the area above, inside or below the envelope represented sub-additive, additive or supra-additive interaction of the 2 agents, respectively.

Establishment of cisplatin-resistant and pemetrexed-resistant cell lines. After subconfluent culture, cells were trypsinized and diluted with complete medium containing cisplatin or pemetrexed for 48 h, until removal of the agents by washing twice with complete medium; this was followed by additional culture for 10-14 days in complete medium alone to obtain drug-resistant colonies large enough for cloning. The isolated colonies were mixed together for propagation to the next passage. This procedure was repeated with gradually increasing concentrations of cisplatin or pemetrexed and continued for ~6 months. The starting concentration was 0.1 μg/ml for both agents; the final cisplatin concentrations were 40, 10, 1 and 5 μg/ml for H2452, H28, H226 and 211H, respectively, and the final pemetrexed concentrations were 10,000, 1, 10 and 5,000 μg/ml for H2452, H28, H226 and 211H, respectively. These resistant sublines were proven to be stably resistant even after at least 2 month-culture in drug-free complete medium. The cisplatin-resistant sublines of the 4 parental cell lines were named H2452-C, H28-C, H226-C and 211H-C, respectively. The pemetrexed-resistant sublines were similarly named H2452-P, H28-P, H226-P and 211H-P. The sensitivity of each resistant subline to cisplatin and pemetrexed was determined by performing clonogenic assays.

Quantitative reverse transcriptase-polymerase chain reaction. The expression levels of TS, GARFT and DHFR in the cells were evaluated with quantitative reverse transcriptase-polymerase chain reaction (RT-PCR). Total RNA was obtained from the cultured cells with the RiboPure™ Kit (Ambion Inc., Austin, TX, USA) according to the manufacturer's instructions. The mRNA levels were measured by TaqMan 5'-nuclease fluorogenic quantitative PCR analysis (Applied Biosystems, Foster, CA, USA) and normalized to β-actin levels according to the manufacturer's instructions. The target-specific primer sequence-sets used were 5'-CCTGAATCACATCGAGCC ACT-3' (forward) and 5'-GAAGAATCCTGAGCTTTGGG AA-3' (reverse) for TS, 5'-GGATAGTTGGTGGCAGTTCTG TT-3' (forward) and 5'-TGCATGATCCTTGTCACAAATA

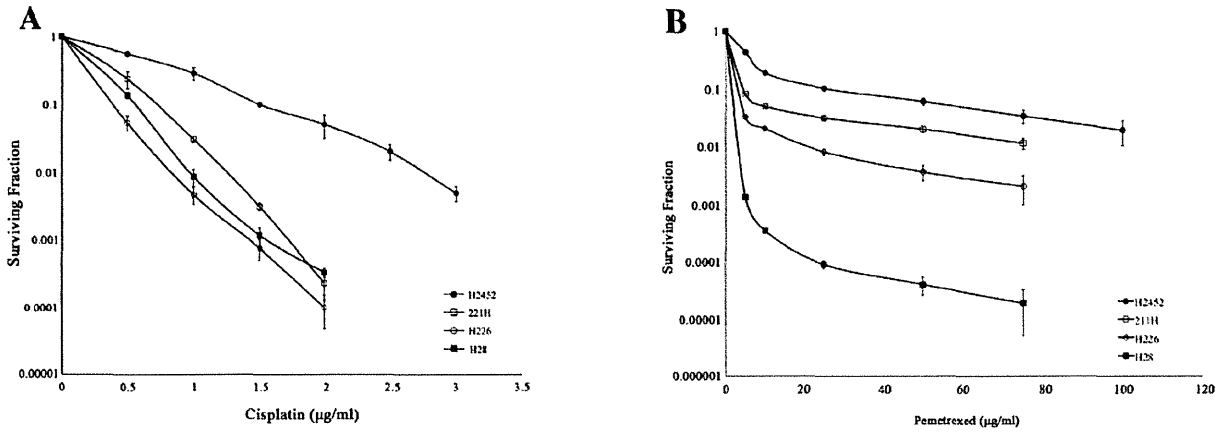

Figure 1. Survival curves for the 4 cell lines treated with cisplatin alone (A) and pemetrexed alone (B). Dots and bars represent mean and SD values, respectively. The mean ± SD of 3 independent experiments, with each sample plated in triplicate, is shown.

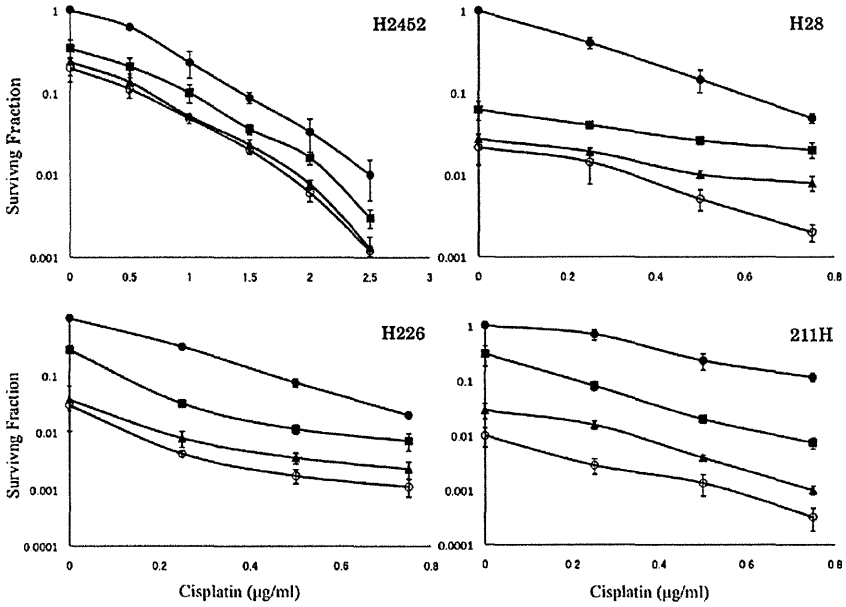

Figure 2. The survival curves for the 4 cell lines treated with a combination of cisplatin and pemetrexed at various concentrations. Concentrations for pemetrexed were 0 (closed circles), 25 (closed squares), 50 (closed triangles) and 75 μg/ml (open circles) in H2452; 0 (closed circles), 0.1 (closed squares), 0.15 (closed triangles) and 0.25 μg/ml (open circles) in H28; 0 (closed circles), 0.5 (closed squares), 1.0 (closed triangles) and 1.5 μg/ml (open circles) in H226; and 0 (closed circles), 1 (closed squares), 3 (closed triangles) and 5 μg/ml (open circles) in 211H. The dots and bars represent mean and SD values, respectively. Each data point represents the mean ± SD of 3 independent experiments in which each sample was plated in triplicate.

GTT-3' (reverse) for DHFR, and 5'-GCTCCCTTCTTTTAAGG GTTCAA-3' (forward) and 5'-ACCAGTAACTGTGACTCC GGT-3' (reverse) for GARFT. The probe sequences were AATTCAGCTTCAGCGAGAACCCAGACC for TS, AAG CCATGAATCACCCAGGCCATCTT for DHFR, and TGC CCATGAGCAAGCCCTGGA for GARFT (14). Quantitative RT-PCR was performed using the ABI PRISM 7000 Sequence Detection System (Applied Biosystems) with the reaction conditions consisting of reverse-transcription at 48°C for 30 min and inactivation of reverse-transcriptase at 95°C for 10 min, followed by 40 cycles of amplification with denaturation at 95°C for 15 sec, annealing and synthesis at 60°C for 60 sec in each cycle.

Statistical analysis. The mRNA levels in the drug-resistant sublines and their parental cell lines were compared and analyzed by the non-parametric Mann-Whitney U test. Differences were judged as statistically significant when p-values (two-tailed) were <0.05.

Results

Survival curves and isobolograms. The survival curves for the cells treated with cisplatin alone and pemetrexed alone are shown in Fig. 1A and B, respectively. Although the remaining 3 cell lines exhibited comparable sensitivity to cisplatin, H2452 was ostensibly more resistant to cisplatin. In addition, it

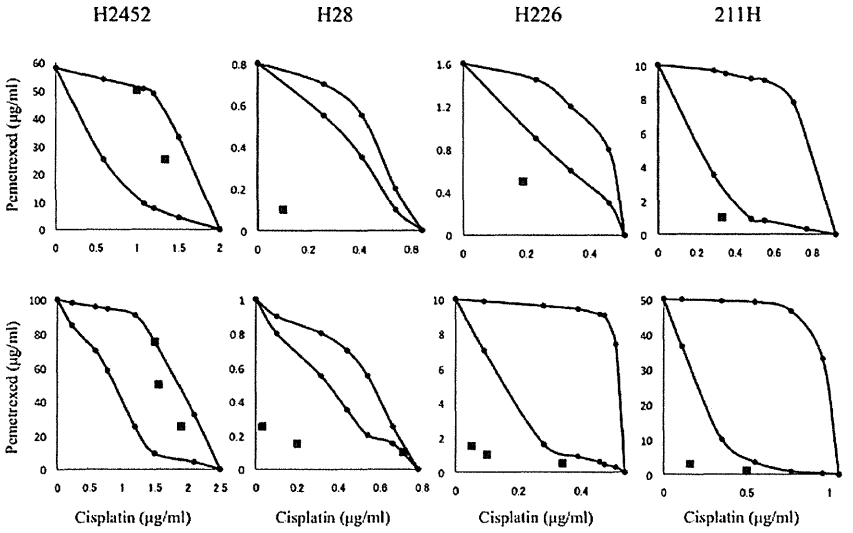

Figure 3. Isobolograms for the 4 cell lines at surviving fractions of 0.05 (top row) and 0.02 (bottom row). In each isobologram, the mode I and II curves were drawn by calculating the theoretical additive response to cisplatin and pemetrexed, resulting in an isobologram envelope. Then, the actual concentrations needed to produce the defined surviving fractions were read directly off the corresponding survival curves shown in Fig. 2 and were plotted on the charts. The interaction of the agents was additive in H2452 and supra-additive in the other 3 cell lines.

Table I. Summary of experimental results.

Phenotype	Cell lines			
	H2542	H28	H226	211H
Baseline sensitivity to cisplatin	Resistant	Sensitive	Sensitive	Sensitive
Baseline sensitivity to pemetrexed	Resistant	Sensitive	Intermediate	Intermediate
Interaction of cisplatin and pemetrexed	Additive	Supra-additive	Supra-additive	Supra-additive
Acquired cisplatin resistance	x10	x100	x100	x10
Acquired pemetrexed resistance	x10	x100	x100	x10
Pemetrexed to cisplatin resistance	Resistant	No	No	No
Cisplatin to pemetrexed resistance	Sensitive	Slight resistant	Slight resistant	No
Baseline TS expression	Intermediate	High	High	Intermediate
TS expression in cisplatin-resistant cells	Decreased	Decreased	Decreased	NS
TS expression in pemetrexed-resistant cells	Increased	Decreased	NS	Increased
Baseline GARFT expression	Intermediate	Intermediate	Low	High
GARFT expression in cisplatin-resistant cells	Decreased	Decreased	Decreased	Decreased
GARFT expression in pemetrexed-resistant cells	Increased	Decreased	NS	Increased
Baseline DHFR expression	Intermediate	High	Low	Low
DHFR expression in cisplatin-resistant cells	NS	Decreased	Decreased	Decreased
DHFR expression in pemetrexed-resistant cells	NS	Decreased	Decreased	NS

NS, not significant.

was also most resistant to pemetrexed. The cells were treated with combinations of cisplatin and pemetrexed at various concentrations, based on the data presented in Fig. 1, to draw the survival curves shown in Fig. 2. The isobologram envelopes for the concentration-combinations that were estimated to produce surviving fractions of 0.05 and 0.02 were drawn for each cell line, as described above. Then, the actual data of concentrations of the agents that produced the same surviving fractions were obtained from Fig. 2 and plotted on the isobologram charts. As shown clearly in Fig. 3, the interaction of cisplatin and pemetrexed was additive for H2452, whereas it was supra-additive or synergistic for the rest of the cell lines.

Sensitivity of the drug-resistant sublines and their cross-resistance. Cisplatin-resistance ratios, determined by the 90% inhibitory concentration (IC_{90}) or IC_{50} when IC_{90} was not deter-

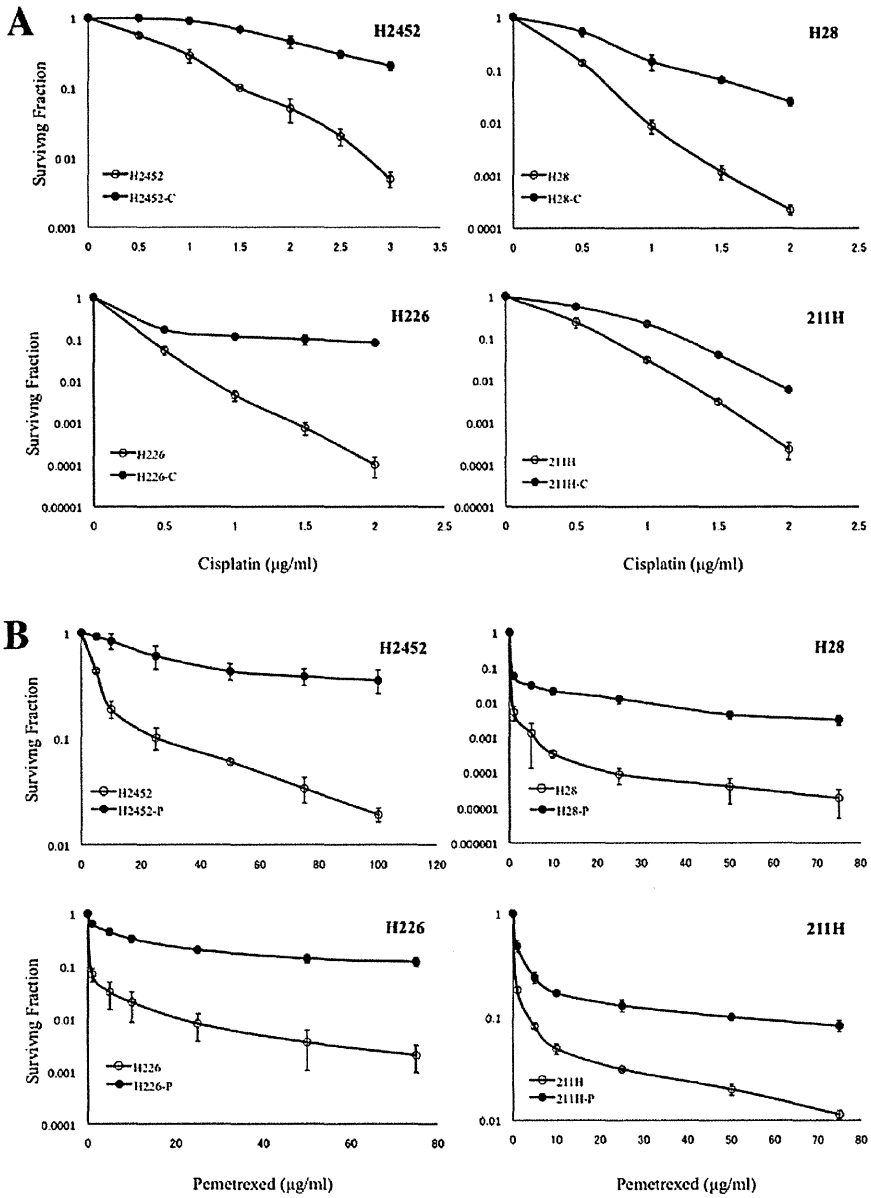

Figure 4. The survival curves for parental cell lines (open circles) and cisplatin-resistant sublines (closed circles) to cisplatin (A), and for parental cell line (open circles) and pemetrexed-resistant subline (closed circles) to pemetrexed (B) in the 4 human MPM cell lines. The dots and bars represent means and SDs, respectively. Each data point represents the mean ± SD of 3 independent experiments in which each sample was plated in triplicate.

mined, of H2452, H28, H226 and 211H were 3.2 (IC_{50} value of 0.60 μg/ml for parental line vs. 1.90 μg/ml for resistant cells), 2.1 (IC_{90} value of 0.56 vs. 1.20 μg/ml), 3.6 (IC_{90} value of 0.39 vs. 1.42 μg/ml) and 1.7 (IC_{90} value of 0.72 vs. 1.25 g/ml), respectively (Fig. 4A). Similarly, pemetrexed-resistance ratios of H2452, H28, H226 and 211H were 9.5 (IC_{50} value of 4 vs. 38 μg/ml), 2.0 (IC_{90} value of 0.25 vs. 0.5 μg/ml), 17.0 (IC_{90} value of 0.2 vs. 3.4 μg/ml) and 14.3 (IC_{90} value of 3.5 vs. 50 μg/ml), respectively (Fig. 4B). Cross-resistance of the 2 agents was investigated by treating cisplatin-resistant sublines with pemetrexed and vice versa, and assessing the results with clonogenic assays. Cisplatin-resistant H2452 (H2452-C) was also resistant to pemetrexed, whereas the other 3 cisplatin-resistant sublines exhibited pemetrexed sensitivities similar to those of their parental lines (Fig. 5A). In contrast, the cisplatin sensitivity in pemetrexed-resistant sublines was significantly diverse. That is, H2452-P was more sensitive, and H28-P and H226-P were less sensitive to cisplatin than their parental cells, whereas 211H-P showed cisplatin-sensitivity indistinguishable from its parental cell line (Fig. 5B).

Expression of TS, GARFT and DHFR in drug-resistant cell lines. Relative mRNA expressions of TS, GARFT and DHFR in the cisplatin-resistant sublines were significantly lower than those in their parental cell lines, except for TS in 211H-C and DHFR in H2452-C (Fig. 6A). In contrast, the expression levels varied widely in pemetrexed-resistant sublines relative to the expression levels in their parental cell lines. The levels of TS and GARFT in H2452-P and 211H-P were significantly higher than those in their parental cells, whereas they were significantly lower in H28-P, with those in H226-P showing

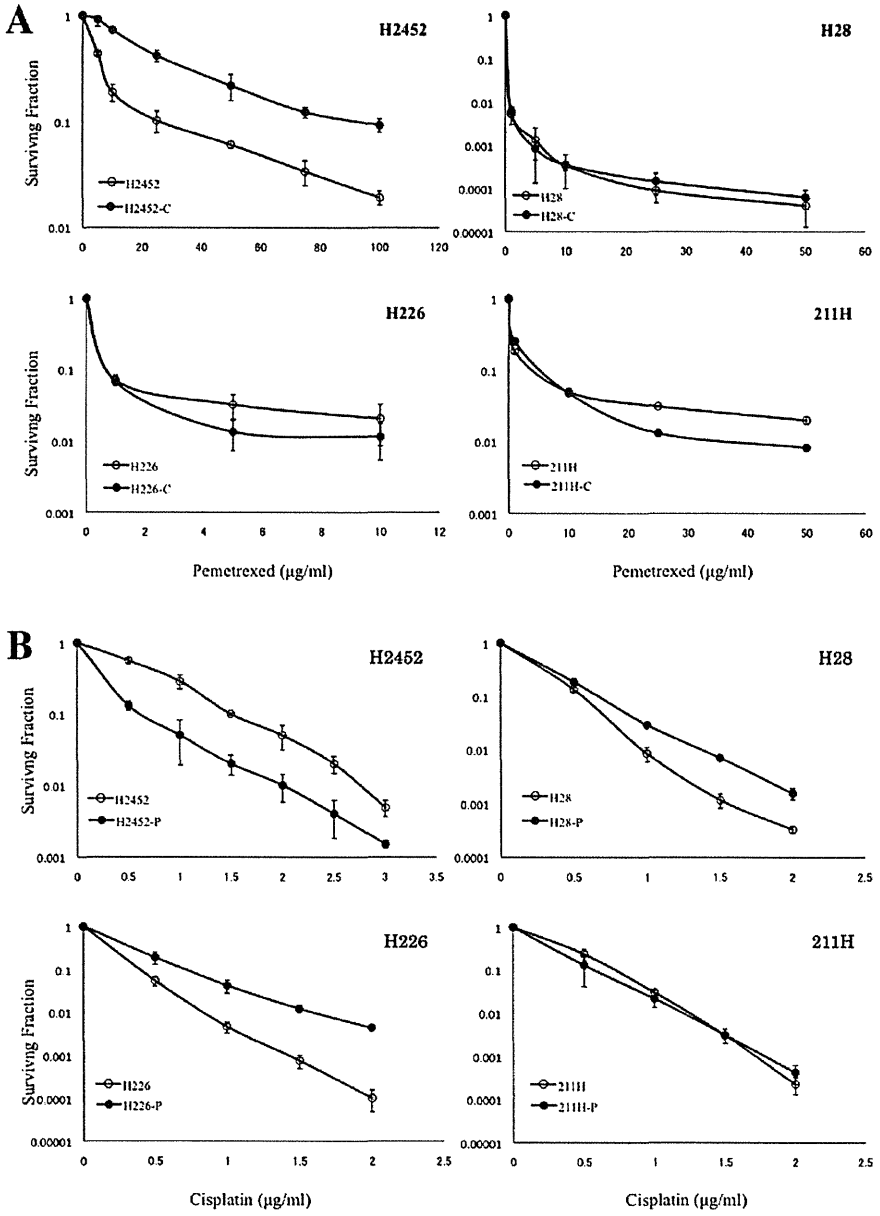

Figure 5. The survival curves for parental cell lines (open circles) and cisplatin-resistant sublines (closed circles) to pemetrexed (A), and for parental cell lines (open circles) and pemetrexed-resistant sublines (closed circles) to cisplatin (B) in the 4 cell lines for investigation of cross-resistance. H2452-C was also resistant to pemetrexed, whereas the other 3 cisplatin-resistant sublines were not resistant to pemetrexed (A). On the other hand, H2452-P was more sensitive, and H28-P and H226-P were moderately less sensitive to cisplatin than their parental cells, whereas 211H-P exhibited similar cisplatin sensitivity as the parental cell lines (B). The dots and bars represent means and SDs, respectively. Each data point represents the mean ± SD of 3 independent experiments in which each sample was plated in triplicate.

no significant change. The DHFR level, however, was significantly lower in H28-P and H226-P, whereas it was not altered significantly in H2452-P and 211H-P (Fig. 6B).

Discussion

In this study, baseline sensitivity to cisplatin and pemetrexed, interaction and cross-resistance of the 2 agents, and altered expression of TS, GARFT and DHFR in cisplatin- and pemetrexed-resistant sublines of 4 human MPM cell lines were investigated. Results generally varied for the 4 cell lines, indicating the heterogeneous and complex nature of MPM in terms of drug sensitivity. However, some common tendencies could be abstracted to characterize the MPM cell lines. As summarized in Table I, the interaction of cisplatin and pemetrexed was synergistic in all the cell lines except one, H2452, which was the most resistant to both the agents. Cross-resistance between the 2 agents was not observed when cisplatin-resistant cells were treated with pemetrexed, except for the cisplatin-resistant H2452-C subline, which was also resistant to pemetrexed. Two of the 4 pemetrexed-resistant cell lines showed mild resistance to cisplatin. The expression

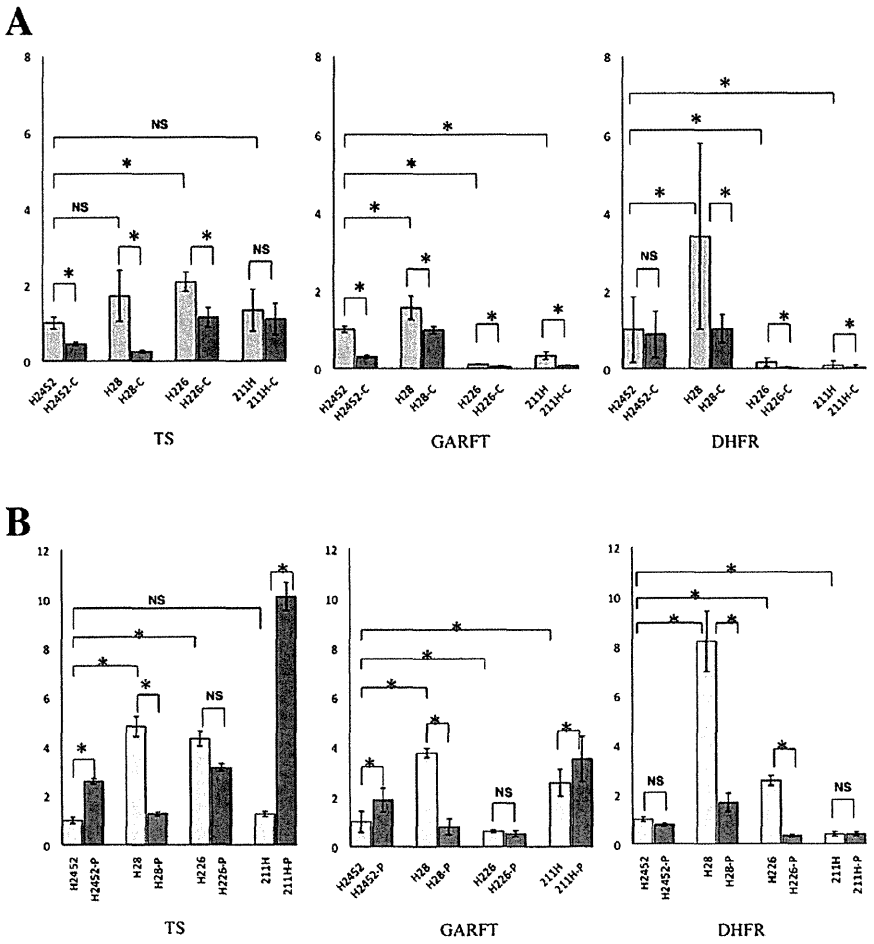

Figure 6. Relative mRNA levels, normalized to β-actin assuming that its expression is equal in the 4 cell lines, of TS, GARFT and DHFR in cisplatin-resistant sublines (A) and in pemetrexed-resistant sublines (B), compared to their levels in parental cells. Columns and bars represent mean and SDs, respectively (n=3). An asterisk represents a statistically significant difference ($p<0.05$) and NS represents not significant.

levels of TS and GARFT were significantly elevated in only 2 of the pemetrexed-resistant sublines, suggesting that resistance mechanisms other than elevated TS expression were likely to be responsible for pemetrexed resistance in the remaining 2 cell lines.

Interaction between cisplatin and pemetrexed has been investigated in cancers other than MPM. Kim *et al* (18) examined 6 gastric cancer cell lines and found that the interaction was supra-additive in 2 and additive in 3 cell lines, with the remaining cell line not described. Kano *et al* (19) investigated the interaction of the 2 agents in 4 human cancer cell lines derived from lung adenocarcinoma and breast, ovarian, and colon cancers, and found that the interaction was schedule-dependent, i.e., simultaneous administration of the 2 agents or sequential administration, with cisplatin followed by pemetrexed, resulted in an additive effect in colon carcinoma and sub-additive effects in the remaining 3 cell lines. However, sequential administration of pemetrexed followed by cisplatin resulted in a supra-additive effect in breast cancer, an additive effect in colon cancer, and a marginal effect between supra-additive and additive in the remaining 2 cell lines. On the other hand, the present study demonstrates a supra-additive effect of cisplatin and pemetrexed in 3 cell lines and an additive effect in 1 human MPM cell line, in accordance with the clinical relevance of combination chemotherapy with the 2 agents for MPM. Cross-resistance between these agents was demonstrated only when 1 of the 4 cisplatin-resistant sublines was treated with pemetrexed, and 2 of the 4 pemetrexed-resistant sublines were treated with cisplatin. These data differ from previous reports on the cross-resistance of these agents in non-small cell lung carcinoma. Zhang *et al* established 4 pemetrexed-resistant sublines from 2 non-small cell lung carcinoma cell lines, and all of them exhibited cross-resistance to cisplatin (21).

A relationship between low TS expression and sensitivity to pemetrexed has been proposed, similar to the correlation between TS expression and the clinical effectiveness of 5-fluorouracil (8-13). In a phase II study where patients with MPM were treated with pemetrexed-based chemotherapy, patients whose tumors showed low TS expression levels showed a significant survival benefit over patients with high TS expression levels (15). Although this implies that TS expression is a prognostic factor, it is not clear if TS expression in tumor tissue relates to sensitivity to the agent. Manipulating TS activity by introducing sense or antisense constructs of the TS gene resulted in reduced pemetrexed sensitivity in non-small cell

carcinoma (16) or augmented pemetrexed sensitivity in MPM (17), respectively. Although these facts seem to provide direct evidence that TS activity is associated with pemetrexed sensitivity, they do not necessarily explain the complete mechanism of natural and acquired resistance to pemetrexed. In fact, the most naturally pemetrexed-resistant cell line, H2452, had the lowest TS expression among the 4 cell lines investigated. In addition, only 2 sublines with acquired pemetrexed resistance had TS expression levels higher than their parental cell lines. Moreover, among the pemetrexed-resistant sublines, H28-P had TS expression level significantly lower than the parental cell line. Although some clinical observations suggest a potential association between low TS expression and response to pemetrexed therapy in breast cancer (14) and MPM (15), a report on gastric cancer cell lines failed to show a correlation between TS expression and pemetrexed sensitivity (18), similar to our observations. Therefore, we assume that multiple mechanisms, including TS expression, are involved in sensitivity to pemetrexed, at least in MPM. A study of colorectal cancer cell lines demonstrated that cell lines with *TP53* mutations were more resistant to antimetabolites, 5-fluorouracil, raltitrexed, and pemetrexed, than cell lines with wild-type *TP53* (22). The fact that *TP53* mutations are infrequent in MPM, and that all the cell lines used in this study possessed wild-type *TP53*, would also explain the differences in the mechanisms of pemetrexed resistance between MPM and other cancers.

Beside the information regarding the drug-drug interaction, cross-resistance and relationship between the drug-resistance and expression of the known relevant, the present research established a useful experimental model for further elucidating mechanism of sensitivity and resistance of these key drugs for MPM. Comprehensive and comparative gene expression analyses using the cell lines established here would be warranted.

In conclusion, cisplatin and pemetrexed have a synergistic effect in human MPM cells and do not show cross-resistance in general. Low TS expression does not necessarily correlate with pemetrexed sensitivity, and elevated TS expression accompanied acquired pemetrexed resistance in only 2 MPM cell lines, suggesting that multiple mechanisms may underlie natural and acquired resistance to pemetrexed in MPM. Further elucidating the underlining mechanism of the present data might uncover molecular targets to treat MPM.

Acknowledgements

This study was funded by grants from the Ministry of Education, Culture, Sports, Science and Technology of Japan.

References

1. Robinson BW and Lake RA: Advances in malignant mesothelioma. N Engl J Med 353: 1591-1603, 2005.
2. O'Brien ME: Malignant mesothelioma - the UK experience. Lung Cancer 45 (Suppl 1): S133-S135, 2004.
3. Niklinski J, Niklinska W, Chyczewska E, *et al*: The epidemiology of asbestos-related diseases. Lung Cancer 45 (Suppl 1): S7-S15, 2004.
4. Tsao AS, Wistuba I, Roth JA and Kindler HL: Malignant pleural mesothelioma. J Clin Oncol 27: 2081-2090, 2009.
5. Vogelzang NJ, Rusthoven JJ, Symanowski J, *et al*: Phase III study of pemetrexed in combination with cisplatin versus cisplatin alone in patients with malignant pleural mesothelioma. J Clin Oncol 21: 2636-2644, 2003.
6. Makimoto T, Tsuchiya S, Nakano H, *et al*: A phase II study of carboplatin-cisplatin-etoposide combination chemotherapy in advanced non-small cell lung cancer. Am J Clin Oncol 20: 51-54, 1997.
7. Shih C, Chen VJ, Gossett LS, *et al*: LY231514, a pyrrolo[2,3-d] pyrimidine-based antifolate that inhibits multiple folate-requiring enzymes. Cancer Res 57: 1116-1123, 1997.
8. Leichman CG, Lenz HJ, Leichman L, *et al*: Quantitation of intratumoral thymidylate synthase expression predicts for disseminated colorectal cancer response and resistance to protracted-infusion fluorouracil and weekly leucovorin. J Clin Oncol 15: 3223-3229, 1997.
9. Metzger R, Danenberg K, Leichman CG, *et al*: High basal level gene expression of thymidine phosphorylase (platelet-derived endothelial cell growth factor) in colorectal tumors is associated with non-response to 5-fluorouracil. Clin Cancer Res 4: 2371-2376, 1998.
10. Salonga D, Danenberg KD, Johnson M, *et al*: Colorectal tumors responding to 5-fluorouracil have low gene expression levels of dihydropyrimidine dehydrogenase, thymidylate synthase, and thymidine phosphorylase. Clin Cancer Res 6: 1322-1327, 2000.
11. Ichikawa W, Uetake H, Shirota Y, *et al*: Combination of dihydropyrimidine dehydrogenase and thymidylate synthase gene expressions in primary tumors as predictive parameters for the efficacy of fluoropyrimidine-based chemotherapy for metastatic colorectal cancer. Clin Cancer Res 9: 786-791, 2003.
12. Ishikawa Y, Kubota T, Otani Y, *et al*: Thymidylate synthetase and dihydropyrimidine dehydrogenase levels in gastric cancer. Anticancer Res 19: 5635-5640, 1999.
13. Huang CL, Yokomise H, Kobayashi S, Fukushima M, Hitomi S and Wada H: Intratumoral expression of thymidylate synthase and dihydropyrimidine dehydrogenase in non-small cell lung cancer patients treated with 5-FU-based chemotherapy. Int J Oncol 17: 47-54, 2000.
14. Gomez HL, Santillana SL, Vallejos CS, *et al*: A phase II trial of pemetrexed in advanced breast cancer: clinical response and association with molecular target expression. Clin Cancer Res 12: 832-838, 2006.
15. Righi L, Papotti MG, Ceppi P, *et al*: Thymidylate synthase but not excision repair cross-complementation group 1 tumor expression predicts outcome in patients with malignant pleural mesothelioma treated with pemetrexed-based chemotherapy. J Clin Oncol 28: 1534-1539, 2010.
16. Takezawa K, Okamoto I, Okamoto W, *et al*: Thymidylate synthase as a determinant of pemetrexed sensitivity in non-small cell lung cancer. Br J Cancer 104: 1594-1601, 2011.
17. Flynn J, Berg RW, Wong T, *et al*: Therapeutic potential of antisense oligodeoxynucleotides to down-regulate thymidylate synthase in mesothelioma. Mol Cancer Ther 5: 1423-1433, 2006.
18. Kim JH, Lee KW, Jung Y, *et al*: Cytotoxic effects of pemetrexed in gastric cancer cells. Cancer Sci 96: 365-371, 2005.
19. Kano Y, Akutsu M, Tsunoda S, *et al*: Schedule-dependent interactions between pemetrexed and cisplatin in human carcinoma cell lines in vitro. Oncol Res 16: 85-95, 2006.
20. Steel GG and Peckham MJ: Exploitable mechanisms in combined radiotherapy-chemotherapy: the concept of additivity. Int J Radiat Oncol Biol Phys 5: 85-91, 1979.
21. Zhang D, Ochi N, Takigawa N, *et al*: Establishment of pemetrexed-resistant non-small cell lung cancer cell lines. Cancer Lett 309: 228-235, 2011.
22. Giovannetti E, Backus HH, Wouters D, *et al*: Changes in the status of p53 affect drug sensitivity to thymidylate synthase (TS) inhibitors by altering TS levels. Br J Cancer 96: 769-775, 2007.

Zoledronic Acid Produces Antitumor Effects on Mesothelioma Through Apoptosis and S-Phase Arrest in p53-Independent and Ras prenylation-Independent Manners

Shinya Okamoto, MS, Kiyoko Kawamura, MS,† Quanhai Li, PhD,† Makako Yamanaka, MD, PhD,†‡ Shan Yang, MS,† Toshihiko Fukamachi, PhD,* Yuji Tada, MD, PhD,‡ Koichiro Tatsumi, MD, PhD,‡ Hideaki Shimada, MD, PhD,§ Kenzo Hiroshima, MD, PhD,‖ Hiroshi Kobayashi, PhD,* and Masatoshi Tagawa, MD, PhD†*

Introduction: We examined whether zoledronic acid (ZOL), the third generation of bisphosphonates, produced cytotoxic effects on human mesothelioma cells in vitro and in vivo, and investigated a possible involvement of p53, Ras, and extracellular signal-regulated kinase1/2 (ERK1/2) pathways.

Methods: Cytotoxicity and cell cycles were assessed with a colorimetric assay and flow cytometry, respectively. Expression levels of apoptosis-linked proteins and prenylation of small guanine-nucleotide-binding regulatory proteins were tested with p53-small interfering RNA, an ERK kinase1/2-inhibitor, and prenyl alcohols. The antitumor activity was examined in an orthotopic animal model.

Results: ZOL treatments suppressed growth of mesothelioma cells bearing the wild-type *p53* gene through apoptosis induction accompanied by activation of caspases, or S-phase arrest by up-regulated cyclin A and B1. ZOL induced p53 phosphorylation and subsequent activation of the downstream pathways. Down-regulated p53 expression with the small interfering RNA, however, showed that both apoptosis and S-phase arrest were irrelevant to the p53 activation. Geranylgeranyl but not farnesyl pyrophosphate inhibited ZOL-induced apoptosis and S-phase arrest, and the geranylgeraniol supplement decreased ZOL-mediated Rap1A but not Ras unprenylation. Inhibition of ERK1/2 pathways suppressed ZOL-induced apoptosis but not S-phase arrest. We further demonstrated that ZOL, administrated intrapleurally, inhibited the tumor growth in the pleural cavity.

Conclusions: These data indicate that ZOL induces apoptosis or S-phase arrest, both of which are independent of p53 activation and Ras unprenylation, and suggest that ZOL is a possible therapeutic agent to mesothelioma partly through non-Ras- and ERK1/2-mediated pathways.

Key Words: Mesothelioma, Bisphosphonate, Small G protein, Prenylation, p53.

(*J Thorac Oncol.* 2012;7: 873–882)

The majority of mesothelioma is associated with asbestos exposure, and data on asbestos consumption predict increased incidences of mesothelioma in industrial countries.[1,2] Approximately 80% of mesothelioma cells have the wild-type (WT) *p53* gene, whereas the INK4A/ARF locus encoding the $p14^{ARF}$ and the 16^{INK4A} genes are commonly deleted.[3,4] Prognosis of mesothelioma is enormously poor, with 6 to 12 months of median survival time after the diagnosis.[5,6] Surgical extrapleural pneumonectomy can be applicable only for the patients in an early clinical phase; mesothelioma cells are generally resistant to radiation and chemotherapeutic agents despite multiple treatment modalities.[1,2,5,6]

Bisphosphonates (BPs) are synthetic analogues of pyrophosphate and have a strong affinity for mineralized bone matrix.[7] BPs can inhibit bone absorption by acting on osteoclasts, and are currently used for bone lesions such as osteoporosis and hypercalcemia. The first generation of BPs stimulates production of nonhydrolyzable cytotoxic adenosine-triphosphate analogues and decreases mitochondrial membrane potential ($\Delta\Psi m$). Conversely, the second and third generations inhibit farnesyl pyrophosphate (FPP) synthetase, a key enzyme in the mevalonate pathways, and deplete isoprenoid pools, which subsequently result in decreased prenylation of small guanine-nucleotide-binding regulatory proteins (small G proteins) (see Supplementary Figure 1, Supplemental Digital Content 1, http://links.lww.com/JTO/A222). The unprenylation influences activities of the small G proteins, which play a crucial role in a variety of biological

*Department of Biochemistry, Graduate School of Pharmaceutical Sciences, Chiba University, Chiba, Japan; †Division of Pathology and Cell Therapy, Chiba Cancer Center Research Institute, Chiba, Japan; ‡Department of Respirology, Graduate School of Medicine, Chiba University, Chiba, Japan; §Department of Surgery, School of Medicine, Toho University, Tokyo, Japan; and ‖Department of Pathology, Tokyo Women's Medical University Yachiyo Medical Center, Yachiyo, Japan.

Disclosure: The authors declare no conflicts of interest.

Address for correspondence: Masatoshi Tagawa, MD, PhD, Division of Pathology and Cell Therapy, Chiba Cancer Center Research Institute, 666-2 Nitona, Chuo-ku, Chiba, Japan 260–8717. E-mail: mtagawa@chiba-cc.jp

ISSN: 1556-0864/12/873-882

functions including cell survival.[8,9] Recent reports demonstrated that BPs produced cytotoxic effects on human tumors by inducing apoptosis and suggested further clinical applications for cancer treatments.[7-9] The detailed mechanisms of cell death, however, remained uncharacterized and a possible p53 involvement in the apoptosis was not well investigated. Several lines of experiments also showed that BPs inhibited Ras activities but contribution of the inhibited Ras actions in cell-growth inhibition was not yet evaluated.[10-12]

In the present study, we examined cytotoxic effects of zoledronic acid (ZOL), one of the third generation of BPs, on human mesothelioma cells and investigated possible antitumor activities in the context of p53 and Ras involvements. We demonstrated that mesothelioma cells were susceptible to ZOL by inducing p53-independent apoptosis or S-phase arrest and that unprenylated Ras was not attributable to the cytotoxic and cytostatic activities. Furthermore, we showed the antitumor effects of ZOL on mesothelioma that developed in the pleural cavity.

MATERIALS AND METHODS

Cells and Mice

Human mesothelioma cells, MSTO-211H, NCI-H28, NCI-H226, NCI-H2052, and NCI-H2452, and immortalized mesothelial cells, Met-5A, were purchased from American Type Culture Collection (Manassas, VA), and JMN-1B, EHMES-1, and EHMES-10 cells were kindly provided by Dr. Hamada (Ehime University, Ehime, Japan).[13] The *p53* status of JMN-1B and EHMES-1 cells are mutated and that of the others including Met-5A are WT, whereas all mesothelioma cells have deficient expressions of $p14^{ARF}$ and $p16^{INK4A}$ resulting from either loss of the transcription or deletion of the genomic DNA (see Supplementary Figure 2, Supplemental Digital Content 2, http://links.lww.com/JTO/A223). In contrast, Met-5A cells have the $p14^{ARF}$ and $p16^{INKA}$ genes. BALB/c *nu/nu* mice (6-week-old females) were purchased from Japan SLC (Hamamatsu, Japan).

Cell Viability Test

Cells were treated with ZOL (Novartis Pharmaceuticals, Tokyo, Japan) alone or together with farnesol (FOH) (Sigma-Aldrich, St. Louis, MO) or geranylgeraniol (GGOH) (Sigma-Aldrich) and for 5 days. Viabilities were assessed with a WST-8 reagent (Dojindo, Kumamoto, Japan) and the amounts of formazan produced were determined with the absorbance at 450 nm (WST assay). The relative viabilities were calculated based on the absorbance without any treatments.

Western Blot Analysis

Lysate from cells treated with ZOL alone or together with FOH, GGOH, or PD98059 (Calbiochem-Merck, Darmstadt, Germany) was subjected to sodium dodecyl sulfate polyacrylamide gel electrophoresis and the protein was transferred to a nitrocellulose membrane, which was further reacted with anti-phospho-p53 at Ser15, anti-caspase-3, anti-cleaved caspase-3, anti-caspase-8, anti-cleaved caspase-8, anti-caspase-9, anti-cleaved caspase-9, anti-Bax, anti-phospho-extracellular signal regulated kinase1/2 (ERK1/2) at Thr202/Tyr204, anti-Bcl-2, (Cell Signaling, Beverly, MA), anti-Mdm2, anti-p21, anti-cyclin A, anti-cyclin B1, anti-unprenylated Rap1A, anti-Rap1 (Santa Cruz Biotechnology, Santa Cruz, CA), anti-Ras, anti-p27 antibodies (BD, San Jose, CA), anti-p53 antibody (Thermo Fisher Scientific, Fremont, CA), or anti-actin antibody (Sigma-Aldrich) as a control followed by an appropriate second antibody. The membranes were developed with the ECL system (GE Healthcare, Buckinghamshire, United Kingdom).

Flow Cytometry

For cell-cycle analysis, cells were fixed with 100% ethanol, treated with 50 μg/ml of RNaseA for 15 minutes, and stained with 50 μg/ml of propidium iodide. For detecting $\Delta\Psi m$, cells were stained with a JC-1 reagent according to the manufacturer's instruction (ImmunoChemistry Technologies, Bloomington, MN) and the fluorescence intensity was analyzed with FACSCalibur and CellQuest software (BD).

Apoptotic DNA Ladder Formation

Genomic DNA was isolated from MSTO-211H cells, untreated or treated with ZOL or cisplatin (CDDP), using an apoptotic DNA ladder kit (Roche Diagnostics, Indianapolis, IN).

RNA Interference

Cells were transfected with small interfering RNA (siRNA) duplex targeting p53 or nonspecific siRNA control (Invitrogen, Carlsbad, CA) for 24 hours using Lipofectamine RNAiMAX according to the manufacturer's protocol (Invitrogen).

Animal Experiments

Cells were injected into the pleural cavity of BALB/c *nu/nu* mice and ZOL or phosphate buffered saline (PBS) as a control was administrated intrapleurally on day 3 or 10. The mice were humanely killed on day 25 or 35, and the tumor weights were measured. The animal experiments were approved by the animal experiment and welfare committee at Chiba University and were performed according to the guideline on animal experiments.

RESULTS

Cytotoxic Activities of ZOL

We examined cytotoxic activities of ZOL in eight human mesothelioma cells and in immortalized Met-5A mesothelial cells with the WST assay (Fig. 1*A*). All of the cells were more sensitive to ZOL than pancreatic carcinoma PANC-1 cells, which were demonstrated to be susceptible to ZOL.[14] The IC_{50} values of ZOL in all the human mesothelioma cells tested and Met-5A cells were less than 10 μM, whereas those in other human tumors were reported as 10 to 85 μM.[7,11] It is, however, unclear whether mesothelium-derived cells are susceptible to ZOL because Met-5A cells are already immortalized by SV40 T antigen that inactivates p53 functions. We also found that ZOL decreased numbers of MSTO-211H cells and suppressed proliferation rates of EHMES-10 cells (see Supplementary

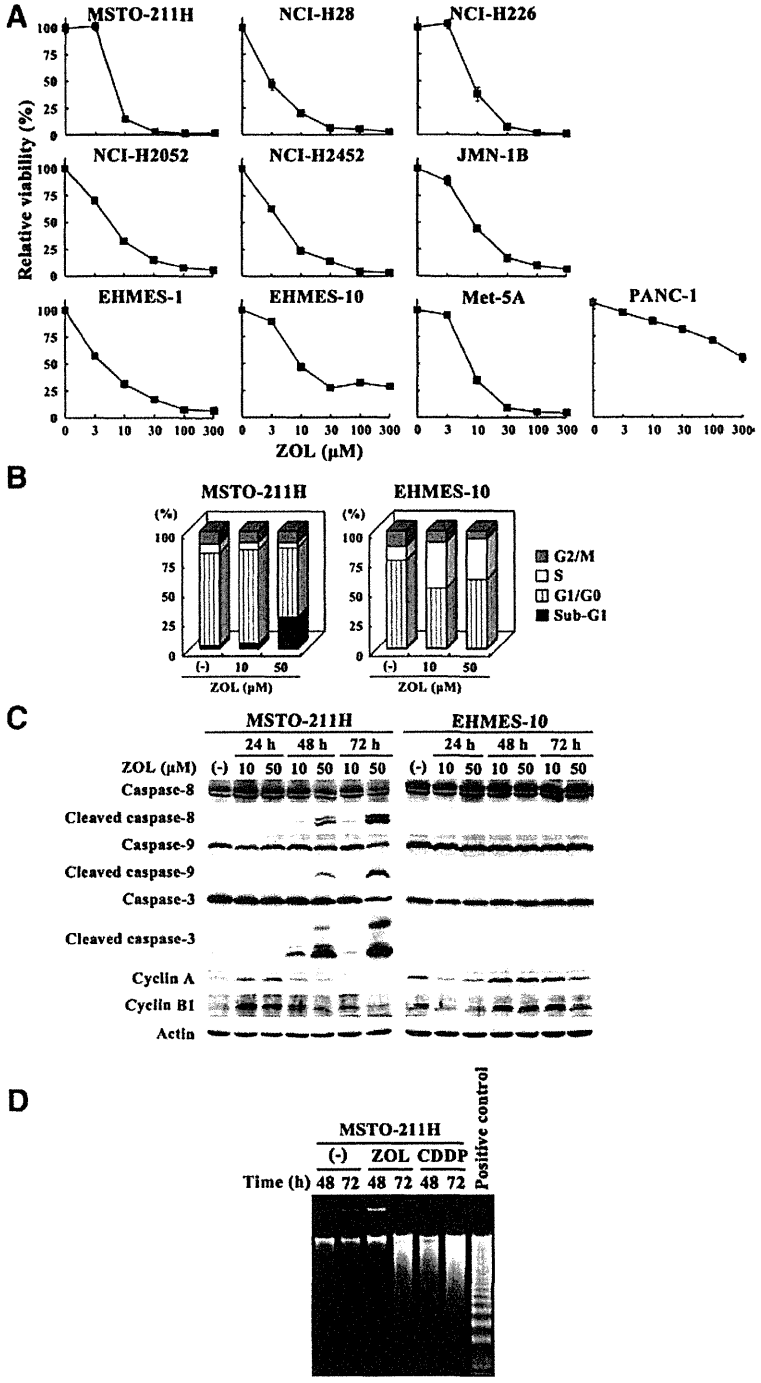

FIGURE 1. Zoledronic acid (ZOL)-induced cytotoxicities by inducing apoptosis or S-phase arrest. (*A*) Cells were treated with ZOL for 5 days and the cell viabilities were measured with the WST assay. The relative viabilities were calculated based on the absorbance without any treatments. Means of triplicated samples and SE bars are shown. (*B*) Flow cytometrical analyses of cell cycles of mesothelioma cells treated with ZOL for 48 hours. (*C*) Western blot analyses to detect caspase cleavages and cyclin expressions in ZOL-treated cells. Cleaved caspases were undetectable in EHMES-10 cells. (*D*) Electrophoresis of genomic DNA from MSTO-211H cells treated with ZOL (50 μM) or CDDP (20 μM). A positive control was DNA of apoptotic U937 cells provided by the manufacturer.

Figure 3, Supplemental Digital Content 3, http://links.lww.com/JTO/A224).

Differential Effects on Cell Cycle and Caspase Activations

We investigated ZOL effects on cell-cycle progression with flow cytometry and found that ZOL treatments increased sub-G1 and S-phase populations depending on the cells tested (Fig. 1*B*). Sequential examinations with different treated periods and concentrations revealed that ZOL treatments induced two characteristic cell-cycle patterns, increased sub-G1 populations without cell-cycle arrest at S phase, which was evidenced in MSTO-211H cells, and augmented S-phase fractions without sub-G1 phase increase in EHMES-10 cells (see Supplementary Table 1, Supplemental Digital Content 4, http://links.lww.com/JTO/A225). Other cells showed an increase of S-phase populations and then that of sub-G1 fractions (for

JMN-1B and EHMES-1 cells, see Supplementary Table 2, Supplemental Digital Content 5, http://links.lww.com/JTO/A226). MSTO-211H and EHMES-10 cells were thus representatives that induced cell death and S-phase arrest, respectively, and were used for further analyses.

We examined expression levels of caspases and cyclin molecules that were associated with cell death and S-phase arrest with Western blot analyses (Fig. 1*C*). Caspase-8 and caspase-9, which are linked with the extrinsic and the intrinsic apoptosis pathways, respectively, were cleaved in ZOL-treated MSTO-211H cells and the respective uncleaved caspase expressions accordingly decreased. Caspase-3 was likewise cleaved with decreased uncleaved caspase-3 expression levels. These caspase cleavages in MSTO-211H cells were observed after 48 hours when sub-G1 populations increased (see Supplementary Table 1, Supplemental Digital Content 4, http://links.lww.com/JTO/A225) and we detected the apoptotic DNA ladders thereafter (Fig. 1*D*). In contrast, ZOL did not or minimally activated the caspases in EHMES-10 cells (also see Fig. 2*D*) but increased expression levels of cyclin A and B1 that were markers of S-phase arrest.[15] MSTO-211H cells also showed transient increase of cyclin A and B1 expressions at 24 hours and the decrease thereafter in accordance with no arrest at S phase.

Induction of Apoptosis and S-Phase Arrest in a p53-Independent Manner

We examined a possible activation of p53 pathways in MSTO-211H and EHMES-10 cells (Fig. 2). We firstly demonstrated that CDDP treatments caused p53 phosphorylation at Ser15 residue, an activation marker of p53 pathways, and caspase-3 cleavage in both cells (Fig. 2*A*), demonstrating that the p53 downstream pathways were functional.[3] These cells were then subjected to apoptotic cell death (data not shown). ZOL treatments also induced phosphorylated p53 at Ser15 in both cells although up-regulation of p53 expression levels was observed only in EHMES-10 cells (Fig. 2*B*). Further examinations also showed elevated expression levels of p53 targets,[16,17] cleaved Mdm2 at 60 kDa, Bax, and Bcl-2, whereas p21 levels were not up-regulated or even suppressed in EHMES-10 cells (also see Fig. 2*D*). MSTO-211H cells also showed increased p27 expression but EHMES-10 cells did not. Increased expressions of these p53 targets were not completely concordant with the p53 phosphorylation process and, moreover, rather preceded the phosphorylation, particularly in EHMES-10 cells. The treatment at 50 μM for 72 hours induced cell death in MSTO-211H cells and subsequently expression levels of these p53-related proteins including p21 were down-regulated. Attenuated p21 expressions in EHMES-10 cells might be accompanied by the ZOL-induced S phase. In addition, reverse transcription-polymerase chain reaction assays showed that ZOL increased transcripts of p53-target genes, *Puma* and *Noxa* (data not shown) in both cells. These data suggested that ZOL treatments activated p53 and the downstream pathways, although the activation was dependent on cells.

JMN-1B and EHMES-1 cells contain a mutation in the *p53* gene at G245 and R273, respectively, which are mapped

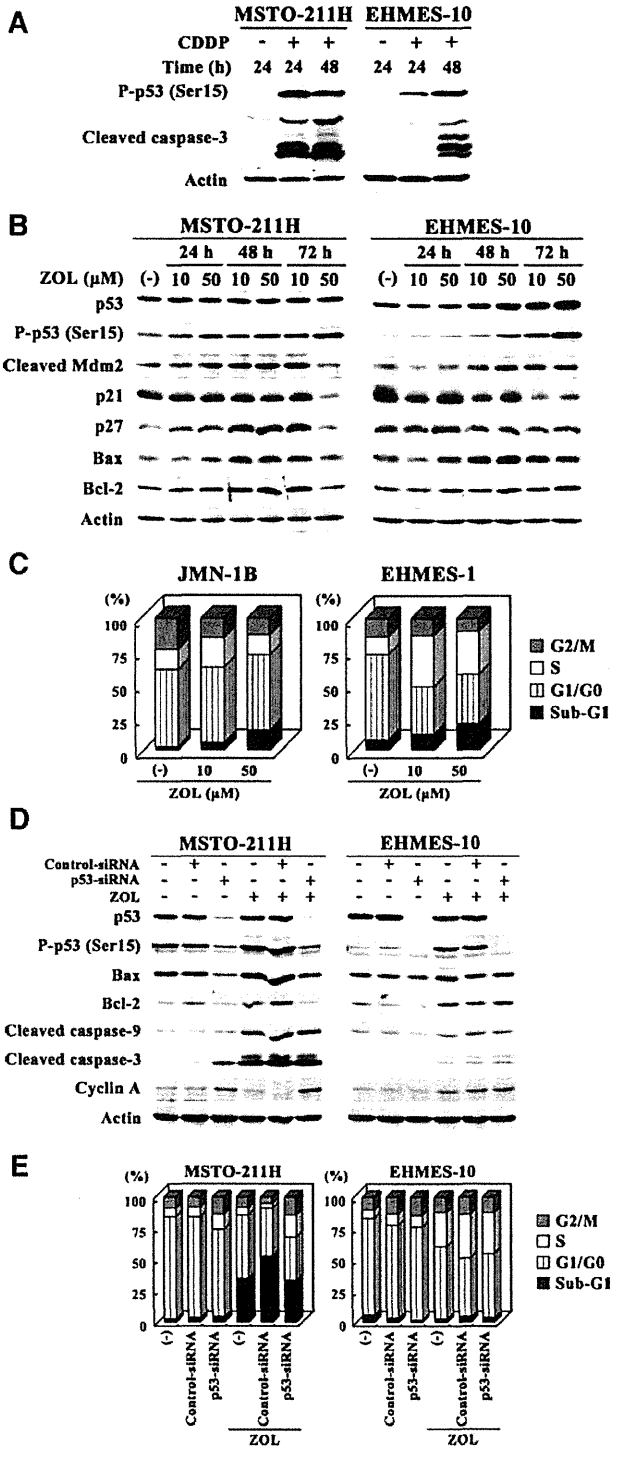

FIGURE 2. Zoledronic acid (ZOL)-mediated p53 activation and small interfering RNA (siRNA)-mediated p53 down-regulation. (*A, B*) Cells were treated with (*A*) CDDP (20 μM) or (*B*) ZOL and then subjected to Western blot analyses. (*C*) Cell-cycle analyses of p53-mutated mesothelioma cells 48 hours after ZOL treatments. (*D, E*) Cells were transfected with 5 nM p53-siRNA or nonspecific control-siRNA for 24 hours and then treated with 50 μM ZOL for 48 hours. They were subjected to (*D*) Western blot analyses or (*E*) cell-cycle analyses.

to a frequent mutation site within the DNA-binding region.[18] The cell lines were as sensitive to ZOL as the other *p53* WT mesothelioma cells (Fig. 1*A*) and ZOL treatments induced S-phase arrest and subsequent apoptotic cell death (Fig. 2*C* and see Supplementary Table 2, Supplemental Digital Content 5, http://links.lww.com/JTO/A226), suggesting that p53 activation was not essential for the cytotoxic effects by ZOL.

We further investigated p53 involvements in the apoptosis and the S-phase arrest by silencing p53 with p53-specific siRNA (Fig. 2*D* and 2*E*, and see Supplementary Table 3, Supplemental Content 6, http://links.lww.com/JTO/A227). Transfection of p53-siRNA suppressed p53 expression levels and inhibited the phosphorylation irrespective of ZOL treatments. Expressions of p53 target molecules, Bax and Bcl-2, were accordingly down-regulated in ZOL-untreated cells. ZOL-induced up-regulated expressions of Bax and Bcl-2 decreased with the siRNA treatments in MSTO-211H cells but ZOL-mediated cleavages of caspase-9 and -3 were not influenced. Introduction of siRNA alone increased cyclin-A expressions in MSTO-211H cells probably because inhibiting endogenous p53 resulted in cell-cycle progression, and in fact temporally increased the S-phase fraction (see Supplementary Table 3, Supplemental Digital Content 6, http://links.lww.com/JTO/A227) and the cell proliferation (data not shown). Expressions of Bax, Bcl-2, cleaved caspase-9 and -3, and cyclin A in ZOL-treated EHMES-10 cells were not affected by the siRNA treatments, suggesting that the ZOL-mediated expression changes were not regulated by p53 in EHMES-10 cells. Cell-cycle analyses demonstrated that the siRNA transfection did not influence ZOL-mediated increase of sub-G1 populations in MSTO-211H cells or S-phase fractions in EHEMS-10 cells (Fig. 2*E*, Supplementary Table 3, http://links.lww.com/JTO/A227). These data collectively suggested that ZOL-induced cytotoxic and cytostatic effects on human mesothelioma cells were independent of the p53 activation. Control-siRNA increased ZOL-mediated increase of sub-G1 populations in MSTO-211H with minimally influencing the expression levels of Bax, caspase-9 or -3, and cyclin A, but the mechanism is currently unknown.

Involvement of Unprenylated Small G Proteins

We examined the possible involvement of unprenylated small G proteins in ZOL-induced cytotoxicities (Fig. 3*A*). ZOL treatments increased unprenylated forms of Ras and Rap1A, which migrated as a higher molecular mass, in MSTO-211H cells. In contrast, the ZOL-treated EHMES-10 cells showed Rap1 but not Ras unprenylation. We further examined the biological role of the unpreylation in ZOL-induced effects with isoprenoid precursors (Fig. 3*B*). FOH and GGOH, membrane-permeable agents, can be converted into isoprenoid, FPP, and geranylgeranyl pyrophosphate, respectively, and thus both agents become substrates for the prenylation, farnesylation and geranylgeranylation of small G proteins (see Supplementary Figure 1, Supplemental Digital Content 1, http://links.lww.com/JTO/A222). FOH treatments inhibited ZOL-induced Ras but not Rap1A unprenylation or p53 phosphorylation at Ser15. FOH at 10 μM did not influence the ZOL-induced cleavage levels of caspase-9 or -3 but the treatment at 30 μM minimally enhanced the cleavage in MSTO-211H, which could be because of FOH toxicity. GGOH-treated MSTO-211H cells, however, showed complete inhibition of ZOL-induced Rap1A unprenylation, p53 phosphorylation at Ser15 and the caspase cleavages, and, interestingly, increase of Ras unprenylation. ZOL-induced down-regulation of cyclin A was inhibited by GGOH but not by FOH in MSTO-211H cells. Likewise, FOH at 10 μM did not influence the ZOL-induced Rap1A prenylation, p53 phosphorylation, or cyclin-A expression, but GGOH at 10 μM inhibited these ZOL-mediated effects in EHMES-10 cells. FOH at 30 μM, however, inhibited the Rap1A unprenylation and the p53 phosphorylation in EHMES-10 cells. GGOH at 30 μM could be toxic to EHMES-10 cells and cleaved the caspase-9 in a manner similar to FOH at 30 μM in MSTO-211H cells. GGOH also induced Ras unprenylation in ZOL-treated EHMES-10 cells as found in MSTO-211H cells.

We also investigated effects of the isoprenoid precursors with the WST assay and flow cytometry (Fig. 3*C* and 3*D*). Incubation with GGOH but not FOH inhibited ZOL-mediated suppression of cell viabilities in MSTO-211H and EHMES-10 cells. GGOH also reverted ZOL-mediated increase of sub-G1 populations in MSTO-211H cells, and S-phase arrest in EHMES-10 cells (see Supplementary Table 4, Supplemental Digital Content 7, http://links.lww.com/JTO/A228). We examined the possible involvement of mitochondria-mediated apoptosis pathways in MSTO-211H cells with a JC-1 agent that represented $\Delta\Psi m$ (Fig. 3*E*). ZOL treatments reduced the JC-1 fluorescence intensity in a dose-dependent manner and GGOH treatments restored the decreased $\Delta\Psi m$ induced by ZOL. These data collectively suggested that GGOH but not FOH inhibited ZOL-induced effects and that the apoptosis and cell-cycle changes were attributable to unprenylated geranylgeranylation of small G proteins excluding Ras.

ERK1/2 Pathways Linked with Apoptosis but not with S-Phase Arrest

We examined the possible involvement of ERK1/2 pathways in the ZOL-mediated pathways (Fig. 4*A*). We first confirmed that epidermal growth factor induced phosphorylation of ERK1/2 in both MSTO-211H and EHMES-10 cells,[19] which suggested that the upstream pathways of ERK1/2 were maintained in both cells (see Supplementary Figure 4, Supplemental Digital Content 8, http://links.lww.com/JTO/A229). PD98059, an inhibitor of ERK kinase1/2 (MEK1/2), which was located in an upstream site of ERK1/2,[20] inhibited endogenous ERK1/2 phosphorylation in both MSTO-211H and EHMES-10 cells. ZOL treatments decreased ERK1/2 phosphorylation in MSTO-211H cells but, interestingly, increased the phosphorylation in EHMES-10 cells. Treatments with PD98059 before treatments with ZOL further decreased the phosphorylation in MSTO-211H cells and inhibited the ZOL-induced augmented phosphorylation in EHMES-10 cells. PD98059 increased p53 expression levels and the phosphorylation in ZOL-untreated but not ZOL-treated EHMES-10 cells and minimally influenced the levels in MSTO-211H cells.

We then examined whether ERK1/2 down-regulation influenced the ZOL-induced cell-cycle progressions (Fig. 4*B*). PD98059 alone did not markedly influence the cell cycle,

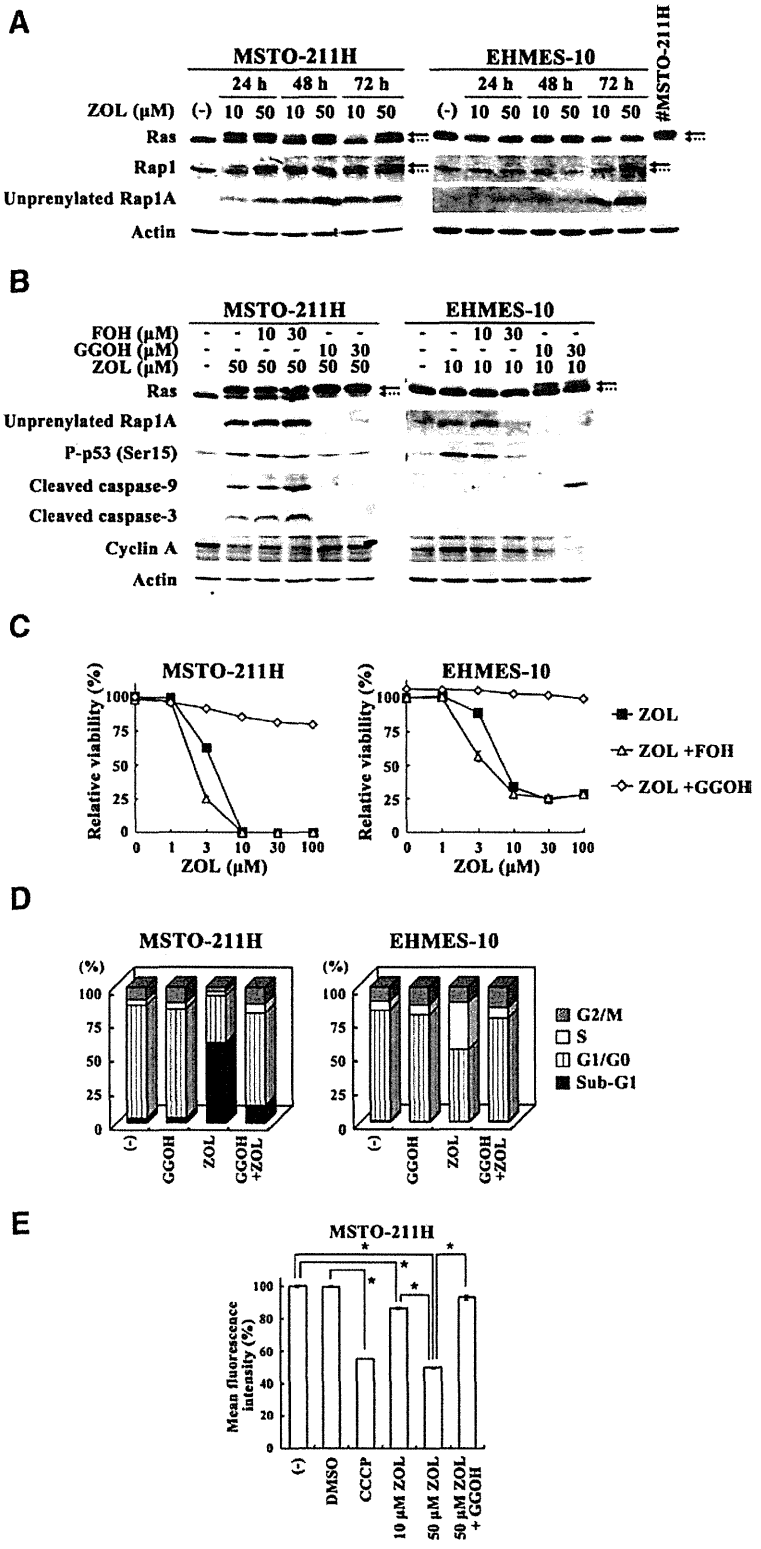

FIGURE 3. Geranylgeranylated small G proteins were involved in zoledronic acid (ZOL)-induced effects. (*A, B*) Cells were treated with (*A*) ZOL or (*B*) first treated with farnesol (FOH) or geranylgeraniol (GGOH) for 3 hours and then with ZOL for 48 hours in MSTO-211H cells or for 72 hours in EHMES-10 cells. The cell lysate was subjected to Western blot analyses. Two bands with high (arrow) and low (dotted arrow) molecular weights correspond to unprenylated and prenylated form of Ras and Rap1A. #MSTO-211H cells treated with 50 μM ZOL for 24 hours as a control. (*C*) Cells were treated with various concentrations of ZOL alone or together with 10 μM GGOH or FOH for 5 days and the relative viabilities were measured with the WST assay. Means of triplicated samples with SE bars are shown. (*D*) Cell-cycle analyses of cells treated with 50 μM ZOL or 10 μM GGOH alone, or both agents together for 48 hours. (*E*) Flow cytometrical analyses for $\Delta\Psi m$. Cells were first treated with GGOH for 3 hours and then with ZOL for 48 hours. Cells were also treated with 0.1% dimethyl sulfoxide as a solvent control or with 50 μM carbonyl cyanide m-chlorophenyl hydrazone (CCCP) for 1 hour as a control for mitochondrial depolarization. Means of triplicated samples with SE bars are shown. $*p < 0.01$.

although PD98059 treatments inhibited ZOL-mediated increase of sub-G1 populations in MSTO-211H cells (see Supplementary Table 5, Supplemental Digital Content 9, http://links.lww.com/JTO/A230). PD98059, however, did not affect the ZOL-induced S-phase arrest in EHMES-10 cells. In accordance with the cell cycle, PD98059 suppressed caspase-9 and -3 cleavages in MSTO-211H cells but did not influence cyclin-A expression levels in EHMES-10 cells (Fig.

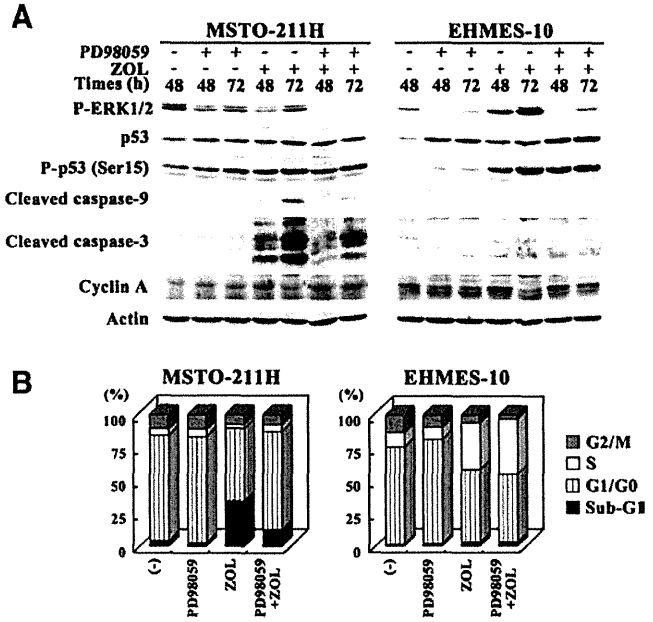

FIGURE 4. PD98059 effects on zoledronic acid (ZOL)-induced apoptosis and S-phase arrest. (*A, B*) Cells were treated with 20 μM PD98059 for 2 hours and then further treated with 50 μM ZOL for 48 or 72 hours. They were subjected to (*A*) Western blot analyses or (*B*) cell-cycle analyses (data at 48 hours are shown).

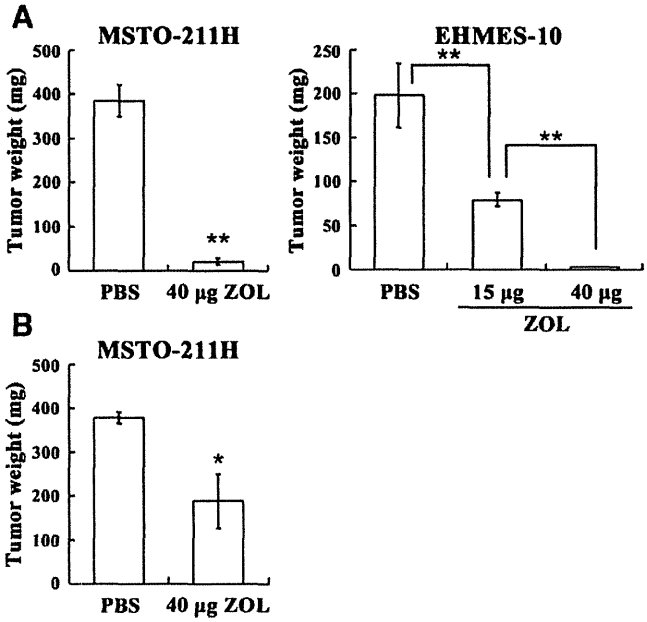

FIGURE 5. Zoledronic acid (ZOL)-mediated antitumor effects in an orthotopic animal model. (*A, B*) Cells (1×10^6) were inoculated into the pleural cavity in BALB/c *nu/nu* mice and then ZOL or phosphate buffered saline (PBS) as a control was intrapleurally administered on (*A*) day 3 or (*B*) 10. (*A*) Tumor weights were measured on day 25 (MSTO-211H cells) or 35 (EHMES-10 cells) ($n = 6$ or 7). (*B*) Some of the mice intrapleurally injected with MSTO-211H cells ($n = 6$) were confirmed to bear the tumor development on day 10. The rest of mice were treated with ZOL ($n = 8$) or PBS ($n = 7$) on day 10 and were examined for the tumor weight on day 25. SE bars are also shown. $*p < 0.05$, $**p < 0.01$.

4*A*). These data demonstrated that ERK1/2 pathways mediated the ZOL-induced apoptosis but were irrelevant to the S -phase arrest although PD98059 inhibited the ERK1/2 phosphorylation in both cells.

Inhibited Tumor Development In vivo

We investigated ZOL-induced antitumor effects in an orthotopic animal model with two treatment schedules (Fig. 5). Nude mice were injected with mesothelioma cells in the pleural cavity and received ZOL treatment intrapleurally. All the tumors were found in the pleural cavity without any detectable metastatic foci. Administration of 40-μg ZOL on day 3 inhibited the tumor growth in mice injected with MSTO-211H or EHMES-10 cells in comparison with the PBS-injected group, and the inhibition was in a dose-dependent manner (Fig. 5*A* and see Supplementary Figure 5, Supplemental Digital Content 10, http://links.lww.com/JTO/A231). As the second model, we injected 40-μg ZOL into the mice on day 10. Some of the mice in the second model were humanely killed on day 10 after tumor inoculation and the tumor development (35 mg in average) was confirmed in all the mice examined. The delayed ZOL administration diminished the antitumor effects but the inhibitory effects of ZOL were also produced compared with PBS injection (Fig. 5*B*). We also examined possible apoptosis in vivo with the terminal deoxynucleotidyl transferase-mediated dUTP nick end labeling assay but failed to detect ZOL-induced apoptotic MSTO-211 cells (data not shown) probably because of a rapid clearance of the apoptotic cells in in vivo settings.

DISCUSSION

In this study we showed that ZOL produced antitumor effects on mesothelioma in vitro and in vivo and demonstrated that the ZOL-induced apoptosis and S-phase arrest were independent of the p53 pathways although ZOL activated p53 pathways. The present study also suggested that the apoptosis and the cell-cycle arrest were attributable to increased unprenylated small G proteins excluding Ras and that the ERK1/2 pathways were involved in the apoptosis.

The majority of human mesothelioma possesses the WT *p53* gene but often lacks the $p14^{ARF}$ and the 16^{INK4A} genes, which subsequently suppresses the p53 and the pRb pathways, respectively.[3,4] ZOL treatments up-regulated p53 expression levels and the phosphorylation, and enhanced the expression levels of p53 downstream molecules such as Bax and cleaved Mdm2. These data implied that the p53 activation could be involved in the apoptosis and the S-phase arrest. Transfection of p53-siRNA, however, did not influence the ZOL-induced cell-cycle changes, cleavage of caspase-3 and -9 expressions in apoptotic cells, or cyclin-A expression in S-phase arrested cells. In addition, p53-mutated mesothelioma cells were also susceptible to the ZOL-induced S-phase arrest and subsequently apoptosis. Time courses of the p53 activation were

not completely matched to the cell-cycle changes. These data collectively indicated that p53 activation did not contribute to ZOL-induced apoptosis or S-phase arrest although Bax and Bcl-2 expressions were regulated by p53 levels. The p53 involvements in ZOL-induced cytotoxicity have been controversial but previous studies mentioning the p53-independent ZOL-mediated activities merely compared the cytotoxicity between *p53* WT and the mutated cells.[21 23] The present study, however, first demonstrated the irrelevance of p53 by down-regulating p53 with the specific siRNA. Nevertheless, the biological significance of ZOL-induced p53 activation and the mechanism remain uncharacterized. The p53 activation could possibly be a consequence of cell death or S-phase arrest. Moreover, the present study suggests that phosphorylation of p53 is subjected to a variety of factors.[24,25] Unprenylated small G proteins excluding Ras play a certain role in the ZOL-induced p53 activation, but the ERK1/2 pathways were irrelevant to ZOL-induced p53 regulations because PD98059 treatments did not influence p53 or the phosphorylation levels in ZOL-treated cells. The pathways themselves can, however, be involved in the p53 regulations because PD98059 up-regulated p53 and the phosphorylation levels in ZOL-untreated EHMES-10 cells.

ZOL-induced unprenylation and isoprenoid precursors-induced reprenylation were dependent on small G proteins and cells tested. Rap1A was unprenylated in both ZOL-treated MSTO-211H and EHMES-10 cells, but Ras unprenylation was observed only in MSTO-211H cells. FOH treatments did not influence prenylation of Rap1A except at a high concentration in EHMES-10 cells but GGOH completely inhibited Rap1A unprenylation. In contrast, GGOH rather increased Ras unprenylation in both cells. Prenlyation of Ras and Rap1A were farnesylation and geranylgeranylation processes, respectively,[26–28] and consequently FPP (FOH equivalent) and geranylgeranyl pyrophosphate (GGOH equivalent) induced reprenylation of Ras and Rap1A, respectively.[29–34] The present study, however, suggests that FOH can be converted into geranylgeranyl pyrophosphate in EHMES-10 cells, which results in differential effects of FOH at 30 μM on inhibiting Rap1A unprenylation observed in between MSTO-211H and EHMES-10 cells. Our data also suggested that GGOH could suppress an activity of the FPP syntase or the upstream enzyme(s), perhaps HMG-CoA reductase, through a possible feedback inhibition and subsequently decreased FPP amounts, which results in GGOH-induced Ras unprenylation.[32] Farnesyl and geranylgeranyl pyrophosphate pool sizes in respective cells and/or regulations of isoprenoid-synthesizing enzymes could differentially influence prenylation processes of small G proteins.

ZOL-induced effects, apoptosis, and S-phase arrest, were inhibited by GGOH but not FOH treatments. ZOL-mediated growth suppression is thus linked with ungeranylgeranylated small G proteins but irrelevant to Ras unprenylation. Determination of non-Ras small G proteins that are responsible for ZOL-mediated growth inhibition is one of the issues to be investigated. ZOL treatments induced morphological changes that could resemble those found in Rho inhibitor-treated cells (see Supplementary Figure 6, Supplemental Digital Content 11, http://links.lww.com/JTO/A232) but it is uncertain whether Rho is involved in cell-growth regulations.[35] The differential effects of FOH and GGOH on ZOL-induced actions are also influenced by the susceptibility of small G proteins to ZOL-mediated unprenylation and by isoprenoid pool levels in the target cells. Nevertheless, GGOH-induced Ras unprenylation and unprenylated Ras-independent apoptosis were first demonstrated in the present study. The biological roles of Ras signaling and Ras mutations in mesothelioma have not been studied in depth, but the current study suggests that mesothelioma cells may be less dependent on Ras activities for their survival.

PD98059 decreased ZOL-induced sub-G1 populations but did not influence the S-phase arrest. The agent also concordantly suppressed capsase-9 and -3 activations but produced little effect on cyclin-A expression. These data suggest that the ERK1/2 pathways could modulate cellular responses by ZOL. Previous studies showed controversial results whether the third generation of BPs activated ERK1/2 pathways[12,22,29] but the present study demonstrated that the ZOL-mediated ERK1/2 regulation depended on the cells tested. ZOL induced dephosphorylation of ERK1/2 in MSTO-211H cells, but enhanced the phosphorylation in EHMES-10 cells. Activation of ERK1/2 in ZOL-treated EHMES-10 cells can be inhibitory to the apoptosis in contrast to apoptotic MSTO-211H cells, but inhibition of ERK1/2 pathways by PD98059 did not have any effect on the cell cycle in EHMES-10 cells. These data collectively implied that ZOL acted on an upstream pathway of the MEK1/2 and that ERK1/2 pathways played a cell-type dependent role in the ZOL-mediated effects in a complex manner.

ZOL induced caspases-mediated apoptosis pathways. Caspase-8 and -9, representatives for extrinsic and intrinsic pathways, respectively, were cleaved and caspase-3 was also activated. Decreased DCm evidently showed the involvement of the mitochondrial intrinsic pathways. Moreover, the caspase-9 cleavage and the suppressed DCm were restored by GGOH treatments, demonstrating that activation of the intrinsic pathways contributed to ZOL-induced apoptosis. Tumor necrosis factor-receptor family proteins, located upstream to the extrinsic pathways, were scarcely expressed in mesothelioma (data not shown). ZOL-induced caspase-8 cleavage therefore could not be caused by the extrinsic pathways but by caspase-3 activation, as found in anticancer agents that induce apoptosis.[36,37] Caspase-8 in mesothelioma was thus alternately activated by mitochondria-mediated intrinsic pathways. Increased Bax expression levels might be linked with decreased DCm, which can be induced in p53-indpendent manner as reported[21] although the siRNA treatments decreased the Bax expression in the present study. ZOL can increase adenosine-triphosphate–analogue concentrations and directly activate intrinsic apoptosis pathways in a similar mechanism as demonstrated in the first generation of BPs.[32]

The precise mechanism of accumulated S-phase populations remained unclear although cyclin A and B1 were up-regulated. Decreased p21 expression could contribute to cell-cycle progression to S phase.[21,31] Previous reports suggested that ZOL induced DNA damages and subsequently ATR/Chk1/Cdc25C or ATM/Chk1/Cdc25A signal transduction

pathways were responsible for intra-S and G2/M checkpoint mechanisms.[21,38] We noticed that ZOL treatments phosphorylated Chk2 but expression levels of Chk1, Cdc25A, Cdc25B, and Cdc25C were not correlated the S-phase arrest (data not shown). Differential mechanisms regarding whether ZOL would induce apoptosis or S-phase arrest in mesothelioma cells need further investigations. The PD98059 experiments could provide us with a clue because the treatment partially inhibited ZOL-induced apoptosis but not S-phase arrest. Recently, Roelofs et al.[39] suggested that selective unprenylation of Rab induced apoptosis but not S-phase arrest. Effects of ZOL on Rab unpreylation and GGOH-mediated Rab prenylation are thereby one of the aspects which future studies need to investigate. Susceptibility to apoptosis in respective cells, which can be determined by a balance between proapoptotic and antiapoptotic activities, may play a role in determining whether the cells are subjected to apoptosis or S-phase arrest. Difference in the endogenous susceptibility in fact can contribute to the cellular difference because the IC_{50} value of CDDP in EHMES-10 was greater than that in MSTO-211H cells (data not shown).

We first demonstrated to the best of our knowledge that ZOL suppressed the growth of human mesothelioma in in vivo settings. Previous studies also showed that murine mesothelioma, developed subcutaneously or in the peritoneal cavity, was treated with ZOL, administrated intratumorally or intraperitoneally.[30,40] In contrast, we demonstrated the ZOL-mediated antitumor effects in an orthotopic experimental model. Previous in vivo studies with other tumor types showed that ZOL administrations were effective to suppress the bone metastatic lesions[8] because BPs were preferentially accumulated in bone tissues with the rapid clearance from serum.[41,42] This BPs property is disadvantageous as a therapeutic agent to tumors developed outside of bone tissues. In fact, we could not observe any growth retardation of subcutaneous MSTO-211H tumors with 15-μg ZOL injected systemically (data not shown), which corresponded to a mouse-equivalent dose of the human dose clinically in use. The same amount administered intrapleurally inhibited orthotopic EHMES-10 tumor growths and MSTO-211H tumors as well (data not shown). Tumors developed in the thoracic cavity can directly be exposed to ZOL, which increases ZOL-mediated cytotoxicities and the clinical benefits. Interestingly, ^{99m}Tc-diphosphate, a bone-scanning agent with a structure similar to that of BPs, accumulated into pleural effusions[43] and was concentrated in mesothelioma.[40] The high affinity of BPs to mesothelium is also beneficial when the agent is administered in the pleural cavity. Moreover, calcification can be one of the features of mesothelioma,[10,44] which are favorable for a possible use of ZOL as the therapeutic agent. Involvement of γ/δ T-cells activation by ZOL can also contribute to the antitumor effects[9,45] although the activation remained uncharacterized in this study. One of the concerns in a clinical application of ZOL is possible adverse reactions caused by the intrapleural administration. We tested the possibility by injecting 40 μg of ZOL into the pleural cavity of naive mice. The mice did not show pleura effusion or growth retardation of the body weight gain (data not shown). We did not detect any histologic changes of mesothelia between PBS-injected and ZOL-injected groups (Supplementary Figure 7, Supplemental Digital Content 12, http://links.lww.com/JTO/A233).

In conclusion, we demonstrated that ZOL was cytotoxic to mesothelioma by inducing apoptosis via the disruption of $\Delta\Psi m$ and subsequent activation of caspases, and by promoting S-phase arrest, both of which were linked with inhibition of geranylgeranylation. Intrapleural administration of ZOL can be a novel therapeutic for mesothelioma treatments and ZOL-mediated up-regulated p53 may produce possible synergistic effects with CDDP,[23] currently used as the first-line agent for mesothelioma.

ACKNOWLEDGMENTS

Supported by Grants-in-Aid for Scientific Research from the Ministry of Education, Culture, Sports, Science and Technology of Japan, a Grant-in-Aid for Cancer Research from the Ministry of Health, Labor and Welfare of Japan, and a Grant-in-aid from the Nichias Corporation. S. O., MS, was supported by G-COE program, Chiba University.

REFERENCES

1. Tada Y, Takiguchi Y, Hiroshima K, et al. Gene therapy for malignant pleural mesothelioma: present and future. *Oncol Res* 2008;17:239–246.
2. Robinson BW, Lake RA. Advances in malignant mesothelioma. *N Engl J Med* 2005;353:1591–1603.
3. Hopkins-Donaldson S, Belyanskaya LL, Simões-Wüst AP, et al. p53-induced apoptosis occurs in the absence of p14(ARF) in malignant pleural mesothelioma. *Neoplasia* 2006;8:551–559.
4. Prins JB, Williamson KA, Kamp MM, et al. The gene for the cyclin-dependent-kinase-4 inhibitor, CDKN2A, is preferentially deleted in malignant mesothelioma. *Int J Cancer* 1998;75:649–653.
5. Robinson BW, Musk AW, Lake RA. Malignant mesothelioma. *Lancet* 2005;366:397–408.
6. Vogelzang NJ, Rusthoven JJ, Symanowski J, et al. Phase III study of pemetrexed in combination with cisplatin versus cisplatin alone in patients with malignant pleural mesothelioma. *J Clin Oncol* 2003;21:2636–2644.
7. Yuasa T, Kimura S, Ashihara E, Habuchi T, Maekawa T. Zoledronic acid - a multiplicity of anti-cancer action. *Curr Med Chem* 2007;14:2126–2135.
8. Green JR. Bisphosphonates: preclinical review. *Oncologist* 2004;9 Suppl 4:3–13.
9. Green JR. Antitumor effects of bisphosphonates. *Cancer* 2003;97 (3 Suppl):840–847.
10. Kawata E, Ashihara E, Nakagawa Y, et al. A combination of a DNA-chimera siRNA against PLK-1 and zoledronic acid suppresses the growth of malignant mesothelioma cells in vitro. *Cancer Lett* 2010;294:245–253.
11. Kuroda J, Kimura S, Segawa H, et al. The third-generation bisphosphonate zoledronate synergistically augments the anti-Ph+ leukemia activity of imatinib mesylate. *Blood* 2003;102:2229–2235.
12. Koshimune R, Aoe M, Toyooka S, et al. Anti-tumor effect of bisphosphonate (YM529) on non-small cell lung cancer cell lines. *BMC Cancer* 2007;7.
13. Nakataki E, Yano S, Matsumori Y, et al. Novel orthotopic implantation model of human malignant pleural mesothelioma (EHMES-10 cells) highly expressing vascular endothelial growth factor and its receptor. *Cancer Sci* 2006;97:183–191.
14. Tassone P, Tagliaferri P, Viscomi C, et al. Zoledronic acid induces antiproliferative and apoptotic effects in human pancreatic cancer cells in vitro. *Br J Cancer* 2003;88:1971–1978.
15. Shapiro GI. Cyclin-dependent kinase pathways as targets for cancer treatment. *J Clin Oncol* 2006;24:1770–1783.
16. Liebermann DA, Hoffman B, Vesely D. p53 induced growth arrest versus apoptosis and its modulation by survival cytokines. *Cell Cycle* 2007;6:166–170.

17. Pochampally R, Fodera B, Chen L, Lu W, Chen J. Activation of an MDM2-specific caspase by p53 in the absence of apoptosis. *J Biol Chem* 1999;274:15271–15277.
18. Petitjean A, Mathe E, Kato S, et al. Impact of mutant p53 functional properties on TP53 mutation patterns and tumor phenotype: lessons from recent developments in the IARC TP53 database. *Hum Mutat* 2007;28:622–629.
19. Jänne PA, Taffaro ML, Salgia R, Johnson BE. Inhibition of epidermal growth factor receptor signaling in malignant pleural mesothelioma. *Cancer Res* 2002;62:5242–5247.
20. Pang L, Sawada T, Decker SJ, Saltiel AR. Inhibition of MAP kinase kinase blocks the differentiation of PC-12 cells induced by nerve growth factor. *J Biol Chem* 1995;270:13585–13588.
21. Ory B, Blanchard F, Battaglia S, Gouin F, Rédini F, Heymann D. Zoledronic acid activates the DNA S-phase checkpoint and induces osteosarcoma cell death characterized by apoptosis-inducing factor and endonuclease-G translocation independently of p53 and retinoblastoma status. *Mol Pharmacol* 2007;71:333–343.
22. Kuroda J, Kimura S, Segawa H, et al. p53-independent anti-tumor effects of the nitrogen-containing bisphosphonate zoledronic acid. *Cancer Sci* 2004;95:186–192.
23. Benassi MS, Chiechi A, Ponticelli F, et al. Growth inhibition and sensitization to cisplatin by zoledronic acid in osteosarcoma cells. *Cancer Lett* 2007;250:194–205.
24. Kruse JP, Gu W. Modes of p53 regulation. *Cell* 2009;137:609–622.
25. Westwood G, Dibling BC, Cuthbert-Heavens D, Burchill SA. Basic fibroblast growth factor (bFGF)-induced cell death is mediated through a caspase-dependent and p53-independent cell death receptor pathway. *Oncogene* 2002;21:809–824.
26. Wennerberg K, Rossman KL, Der CJ. The Ras superfamily at a glance. *J Cell Sci* 2005;118(Pt 5):843–846.
27. Appels NM, Beijnen JH, Schellens JH. Development of farnesyl transferase inhibitors: a review. *Oncologist* 2005;10:565–578.
28. Wright LP Philips MR. Thematic review series: lipid posttranslational modifications. CAAX modification and membrane targeting of Ras. *J Lipid Res* 2006;47:883–891.
29. Iguchi T, Miyakawa Y, Yamamoto K, Kizaki M, Ikeda Y. Nitrogen-containing bisphosphonates induce S-phase cell cycle arrest and apoptosis of myeloma cells by activating MAPK pathway and inhibiting mevalonate pathway. *Cell Signal* 2003;15:719–727.
30. Wakchoure S, Merrell MA, Aldrich W, et al. Bisphosphonates inhibit the growth of mesothelioma cells in vitro and in vivo. *Clin Cancer Res* 2006;12:2862–2868.
31. Romani AA, Desenzani S, Morganti MM, La Monica S, Borghetti AF, Soliani P. Zoledronic acid determines S-phase arrest but fails to induce apoptosis in cholangiocarcinoma cells. *Biochem Pharmacol* 2009;78:133–141.
32. Räikkönen J, Mönkkönen H, Auriola S, Mönkkönen J. Mevalonate pathway intermediates downregulate zoledronic acid-induced isopentenyl pyrophosphate and ATP analog formation in human breast cancer cells. *Biochem Pharmacol* 2010;79:777–783.
33. Hiraga T, Williams PJ, Ueda A, Tamura D, Yoneda T. Zoledronic acid inhibits visceral metastases in the 4T1/luc mouse breast cancer model. *Clin Cancer Res* 2004;10:4559–4567.
34. Shipman CM, Croucher PI, Russell RG, Helfrich MH, Rogers MJ. The bisphosphonate incadronate (YM175) causes apoptosis of human myeloma cells in vitro by inhibiting the mevalonate pathway. *Cancer Res* 1998;58:5294–5297.
35. Bar-Sagi D Hall A. Ras and Rho GTPases: a family reunion. *Cell* 2000;103:227–238.
36. Tang D, Lahti JM, Kidd VJ. Caspase-8 activation and bid cleavage contribute to MCF7 cellular execution in a caspase-3-dependent manner during staurosporine-mediated apoptosis. *J Biol Chem* 2000;275:9303–9307.
37. Engels IH, Stepczynska A, Stroh C, et al. Caspase-8/FLICE functions as an executioner caspase in anticancer drug-induced apoptosis. *Oncogene* 2000;19:4563–4573.
38. Iguchi T, Miyakawa Y, Saito K, et al. Zoledronate-induced S phase arrest and apoptosis accompanied by DNA damage and activation of the ATM/Chk1/cdc25 pathway in human osteosarcoma cells. *Int J Oncol* 2007;31:285–291.
39. Roelofs AJ, Hulley PA, Meijer A, Ebetino FH, Russell RG, Shipman CM. Selective inhibition of Rab prenylation by a phosphonocarboxylate analogue of risedronate induces apoptosis, but not S-phase arrest, in human myeloma cells. *Int J Cancer* 2006;119:1254–1261.
40. Merrell MA, Wakchoure S, Ilvesaro JM, et al. Differential effects of Ca(2+) on bisphosphonate-induced growth inhibition in breast cancer and mesothelioma cells. *Eur J Pharmacol* 2007;559:21–31.
41. Skerjanec A, Berenson J, Hsu C, et al. The pharmacokinetics and pharmacodynamics of zoledronic acid in cancer patients with varying degrees of renal function. *J Clin Pharmacol* 2003;43:154–162.
42. Sato M, Grasser W, Endo N, et al. Bisphosphonate action. Alendronate localization in rat bone and effects on osteoclast ultrastructure. *J Clin Invest* 1991;88:2095–2105.
43. Sandler ED, Hattner RS, Parisi MT, Miller TR. Clinical utility of bone scan features of pleural effusion: sensitivity and specificity for malignancy based on pleural fluid cytopathology. *J Nucl Med* 1994;35:429–431.
44. Raizon A, Schwartz A, Hix W, Rockoff SD. Calcification as a sign of sarcomatous degeneration of malignant pleural mesotheliomas: a new CT finding. *J Comput Assist Tomogr* 1996;20:42–44.
45. Todaro M, D'Asaro M, Caccamo N, et al. Efficient killing of human colon cancer stem cells by γδ T lymphocytes. *J Immunol* 2009; 182:7287–7296.